Electronic Supplementary Material (ESI) for Soft Matter.
This journal is © The Royal Society of Chemistry 2022

Self-assembly of globular proteins with intrinsically disordered protein polyelectrolytes and block copolymers

*Justin M. Horn, Yuncan Zhu, So Yeon Ahn, and Allie C. Obermeyer**

Department of Chemical Engineering, Columbia University, New York, NY 10027

Supporting Information

Table of Contents

S1. Materials and Methods 3
S2. Cloning of prothymosin-α peptides and fusions 3
S3. Protein Expression 5
S4. Protein Purification 5
S5. Microscopy of Bulk Phase PEC's 6
S6. Turbidity Assays 6
S7. Data Processing and Generation of Heatmaps 7
S8. Dynamic Light Scattering (DLS) 7
S9. Size Exclusion Chromatography Multi-Angle Light Scattering (SEC-MALS) 8
S10. Transmission Electron Microscopy (TEM) 8
S11. Figure S1. Electrophoresis analysis of engineered PA Proteins 9
S12. Figure S2. Cloud point determination of elastin-like peptides 10
S13. Figure S3. Light microscopy of PA or ELP-PA variants and GFP(+36) 11
S14. Figure S4. DLS results of ELP-PA and GFP(+36) mixtures at 5 °C 12
S15. Figure S5. SEC-MALS data for ELP-PA WT mixed with GFP(+36) 13
S16. Figure S6. DLS correlation functions for ELP-PA / GFP(+36) mixtures at 5 °C 14
S17. Figure S7. Turbidity assays for PA WT as a function of temperature 15
S18. Figure S8. Turbidity assays for PA K to Q as a function of temperature 16
S19. Figure S9. Turbidity assays for PA K to D/E as a function of temperature 17
S20. Figure S10. Turbidity assays for PA C-term as a function of temperature 18
S21. Figure S11. Turbidity assays for ELP-PA WT as a function of temperature 19
S22. Figure S12. Turbidity assays for ELP-PA K to Q as a function of temperature 20
S23. Figure S13. Turbidity assays for ELP-PA K to D/E as a function of temperature 21
S24. Figure S14. Turbidity assays for ELP-PA C-term as a function of temperature 22

S25. Figure S15. DLS correlation functions as a function of salt concentration for ELP-PA WT / GFP(+36) at 5 °C 23
S26. Figure S16. DLS correlation functions as a function of salt concentration for ELP-PA K to Q / GFP(+36) at 5 °C 24
S27. Figure S17. DLS correlation functions as a function of salt concentration for ELP-PA K to D/E / GFP(+36) at 5 °C 25
S28. Figure S18. DLS correlation functions as a function of salt concentration for ELP-PA C-term / GFP(+36) at 5 °C 26
S29. Figure S19. DLS data for ELP-PA WT / GFP(+36) at 5 °C as a function of salt concentration 27
S30. Figure S20. DLS data for ELP-PA K to Q / GFP(+36) at 5 °C as a function of salt concentration 28
S31. Figure S21. DLS data for ELP-PA K to D/E / GFP(+36) at 5 °C as a function of salt concentration 29
S32. Figure S22. DLS data for ELP-PA C-term / GFP(+36) at 5 °C as a function of salt concentration 30
S33. Figure S23. DLS as a function of temperature for ELP-PA WT / GFP(+36) at f^+ = 0.6 31
S34. Figure S24. DLS as a function of temperature for ELP-PA K to Q / GFP(+36) at f^+ = 0.6 32
S35. Figure S25. DLS as a function of temperature for ELP-PA K to D/E / GFP(+36) at f^+ = 0.6 33
S36. Figure S26. DLS as a function of temperature for ELP-PA C-term / GFP(+36) at f^+ = 0.6 34
S37. References 35

S1. Materials and Methods

Unless otherwise noted, all primers were purchased from Integrated DNA Technologies (IDT), all double-stranded DNA fragments were purchased from TWIST biosciences, and all enzymes and competent cells were purchased from New England Biolabs. DNA purification kits (miniprep, PCR purification and gel purification) were purchased from Qiagen. All media components and chemicals were purchased from Sigma Aldrich or Fisher Scientific and were used as received.

S2. Cloning of prothymosin-α peptides and fusions

The prothymosin-α (PA) peptide sequence was identified using UniProt (UniProtKB - P06454 (PTMA_HUMAN)). Using the wild type sequence as a starting point, three alternative sequences were created: one with all lysines (K) converted to glutamine (Q), one with all lysines (K) converted to glutamate (E) or aspartate (D), and one composed of the final 70 amino acids of the wild type prothymosin-α. For each peptide sequence, a corresponding DNA sequence was generated using a combinatorial codon scrambler to minimize the repetitiveness of the sequence (https://chilkotilab.pratt.duke.edu/codon-scrambler).[1] These sequences were synthesized and cloned into a pET21 plasmid for IPTG-inducible expression in T7-expressing *E. coli* by TWIST Biosciences. To the N-terminus of each prothymosin-α homopeptide, a 6xHis tag followed by a four-amino acid GGSS linker was added for purification by immobilized metal affinity chromatography.

To generate fusion protein block copolymers, a gene encoding the elastin-like polypeptide (ELP) sequence, GVG-$(VPGVG)_{29}$-VPGWP, and an N-terminal 6xHis Tag with a three amino acid SSG linker, was added to the 5' end (N-terminus) of each prothymosin-α gene in a pET21, IPTG-inducible plasmid. A plasmid containing the desired ELP sequence was purchased from Addgene (Plasmid # 67014). The ELP sequence contained a C-terminal GWP sequence to facilitate protein quantification. The GFP(+36) plasmid was made by introducing site-specific mutations to an sfGFP gene, converting neutral and acidic residues on the surface of superfolder GFP to basic amino acids (Arg, Lys), as previously described.[2]

Fusion genes were prepared by HiFi assembly as directed by NEBuilder, with primers purchased from IDT. PCR products for HiFi assembly were produced using Phusion high-fidelity DNA polymerase (Thermo Scientific). DNA purification was performed using QIAquick PCR purification kits from Qiagen. HiFi Assembly was then performed as instructed using NEB HiFi DNA assembly master mix and relevant PCR products. HiFi assembled DNA products were transformed into chemically competent NEB 5-α *E. coli* following the transformation protocol provided by NEB. Transformed plasmids were subsequently isolated using QIAPrep Spin Miniprep Kits, as instructed by Qiagen. Sanger

sequencing of isolated plasmid DNA was performed by Genewiz. Sequence confirmed plasmids were then transformed into NiCo21(DE3) *E. coli*.

Amino Acid Sequences of all 6xHis-tagged PA and ELP-PA Variants:
Mutations to PA are indicated as bold. The ELP sequence is shown in grey.

PA WT:

GHHHHHHGGS SDAAVDTSSE ITTKDLKEKK EVVEEAENGR DAPANGNAEN
EENGEQEADN EVDEEEEEGG EEEEEEEEGD GEEEDGDEDE EAESATGKRA
AEDDEDDDVD TKKQKTDEDD

PA K to Q:

GHHHHHHGGS SDAAVDTSSE ITT**Q**DL**Q**E**QQ** EVVEEAENGR DAPANGNAEN
EENGEQEADN EVDEEEEEGG EEEEEEEEGD GEEEDGDEDE EAESATG**Q**RA
AEDDEDDDVD T**QQ**Q**Q**TDEDD

PA K to D/E:

GHHHHHHGGS SDAAVDTSSE ITT**E**DL**D**E**DD** EVVEEAENGR DAPANGNAEN
EENGEQEADN EVDEEEEEGG EEEEEEEEGD GEEEDGDEDE EAESATG**D**RA
AEDDEDDDVD T**ED**Q**E**TDEDD

PA C-term:

GHHHHHHGGS EENGEQEADN EVDEEEEEGG EEEEEEEEGD GEEEDGDEDE
EAESATGKRA AEDDEDDDVD TKKQKTDEDD

ELP-PA WT:

HHHHHHSSGG VGVPGVGVPG VGVPGVGVPG VGVPGVGVPG VGVPGVGVPG
VGVPGVGVPG VGVPGVGVPG VGVPGVGVPG VGVPGVGVPG VGVPGVGVPG
VGVPGVGVPG VGVPGVGVPG VGVPGVGVPG VGVPGVGVPG VGVPGVGVPG
VGVPGVGVPG WPSDAAVDTS SEITTKDLKE KKEVVEEAEN GRDAPANGNA
ENEENGEQEA DNEVDEEEEE GGEEEEEEEE GDGEEEDGDE DEEAESATGK
RAAEDDEDDD VDTKKQKTDE DD

ELP-PA K to Q:

HHHHHHSSGG VGVPGVGVPG VGVPGVGVPG VGVPGVGVPG VGVPGVGVPG
VGVPGVGVPG VGVPGVGVPG VGVPGVGVPG VGVPGVGVPG VGVPGVGVPG
VGVPGVGVPG VGVPGVGVPG VGVPGVGVPG VGVPGVGVPG VGVPGVGVPG
VGVPGVGVPG WPSDAAVDTS SEITTQDLQE QQEVVEEAEN GRDAPANGNA
ENEENGEQEA DNEVDEEEEE GGEEEEEEEE GDGEEEDGDE DEEAESATGQ
RAAEDDEDDD VDTQQQQTDE DD

ELP-PA K to D/E:

HHHHHHSSGG VGVPGVGVPG VGVPGVGVPG VGVPGVGVPG VGVPGVGVPG
VGVPGVGVPG VGVPGVGVPG VGVPGVGVPG VGVPGVGVPG VGVPGVGVPG
VGVPGVGVPG VGVPGVGVPG VGVPGVGVPG VGVPGVGVPG VGVPGVGVPG
VGVPGVGVPG WPSDAAVDTS SEITTEDLDE DDEVVEEAEN GRDAPANGNA
ENEENGEQEA DNEVDEEEEE GGEEEEEEEE GDGEEEDGDE DEEAESATGD
RAAEDDEDDD VDTEDQETDE DD

ELP-PA C-term:

HHHHHHSSGG VGVPGVGVPG VGVPGVGVPG VGVPGVGVPG VGVPGVGVPG
VGVPGVGVPG VGVPGVGVPG VGVPGVGVPG VGVPGVGVPG VGVPGVGVPG
VGVPGVGVPG VGVPGVGVPG VGVPGVGVPG VGVPGVGVPG VGVPGVGVPG
VGVPGVGVPG WPEENGEQEA DNEVDEEEEE GGEEEEEEEE GDGEEEDGDE
DEEAESATGK RAAEDDEDDD VDTKKQKTDE DD

GFP+36:

HHHHHHGGAS KGERLFRGKV PILVELKGDV NGHKFSVRGK GKGDATRGKL
TLKFICTTGK LPVPWPTLVT TLTYGVQCFS RYPKHMKRHD FFKSAMPKGY
VQERTISFKK DGKYKTRAEV KFEGRTLVNR IKLKGRDFKE KGNILGHKLR
YNFNSHKVYI TADKRKNGIK AKFKIRHNVK DGSVQLADHY QQNTPIGRGP
VLLPRNHYLS TRSKLSKDPK EKRDHMVLLE FVTAAGIKHG RDERYK

S3. Protein Expression

NiCo21(DE3) cells were spread onto an agar plate (100 µg/mL ampicillin, Gold Biotechnology) and incubated at 37 °C overnight. A single colony from the plate was picked and then inoculated into 5 mL sterilized LB media supplemented with 100 µg/mL ampicillin and grown at 37 °C with shaking at 225 rpm overnight. The overnight culture was then used to inoculate 1 L of sterilized LB media supplemented with 100 µg/mL ampicillin. The 1 L culture was grown at 37 °C with shaking at 225 rpm until the optical density at 600 nm was between 0.6-1.0. The 1 L culture was then induced with 1 mL of 1 M isopropyl ß-D-1-thiogalacopyranoside (IPTG, Gold Biotechnology). Induced culture was then incubated at 25 °C with shaking at 225 rpm for 16-20 h before cells were harvested for purification.

S4. Protein Purification

Cells were harvested by centrifugation in a Thermo Scientific Sorvall Legend XTR centrifuge with swinging bucket rotor (Thermo Scientific TX-750) at 4000 rpm for 10 min and collected cell pellets were resuspended in a lysis buffer (ELP-PA fusions and ELP: 50 mM Na_2HPO_4, pH 8.0; GFP(+36), PA polyanions: 50 mM Na_2HPO_4, 1 M NaCl, pH 8.0). The resuspended cell pellets were subjected to one freeze-thaw cycle before lysis

by sonication with a 0.5" probe (Thermo Scientific) at 60% amplitude (cycle – 2 s on, 4 s off) for 10 min. Cell debris was separated from soluble proteins by centrifugation with a fixed angle rotor (Thermo Scientific, Fiberlite F15-8x50cy) at 10,000 rpm for 30 min at 18 ºC. Proteins in the supernatant were collected carefully into a 50 mL tube and then purified using immobilized metal affinity chromatography. For every 1 L of cell culture, 10-15 mL of His-Pur Ni-NTA resin (Thermo Scientific) was used for purification. Resin was equilibrated with lysis buffer as above then incubated with the soluble fraction of the cell lysate for 20 min. Resin was treated with lysis buffer, wash buffer (PA fusions and homopeptides: 50 mM Na_2HPO_4, 35 mM imidazole, pH 8.0; GFP(+36): 50 mM Na_2HPO_4, 1 M NaCl, 35 mM imidazole, pH 8.0), and elution buffer (PA fusions and homopeptides: 50 mM Na_2HPO_4, 250 mM imidazole, pH 8.0; GFP(+36): 50 mM Na_2HPO_4, 1 M NaCl, 250 mM imidazole, pH 8.0) in succession. Fractions of each buffer were collected and analyzed via SDS-PAGE to determine protein purity. Pure fractions were dialyzed into 10 mM tris at pH 7.4 and then concentrated to the desired concentration by centrifugal filtration using Amicon Ultra centrifugal filter units with a 10 kDa molecular weight cutoff (Millipore Sigma). Final protein concentration for PA variants was determined by BCA assay using the Pierce BCA Protein Assay Kit (Fisher Scientific) with a BSA standard. Final protein concentration for GFP(+36) was obtained by measuring the absorbance at 488 nm on a Cary 60 UV-Vis spectrophotometer (Agilent Technologies). This absorbance measurement was converted to concentration using Beer's Law and the extinction coefficient for sfGFP at 488 nm (ε = 8.33 x 10^5 M^{-1} cm^{-1})

S5. Microscopy of Bulk Phase PEC's

Microscopy samples were prepared at a total macromolecule concentration of 0.8 or 1 mg/mL in 10 mM tris at a pH of 7.4 with varying concentrations of NaCl (0-400 mM) in a total volume of 30-50 µL in a 384-well glass bottom plate (Cellvis). Sample preparation was largely the same as described below in S6. Turbidity Assays. Images were taken using an Evos FL Auto 2 optical microscope (Invitrogen) at room temperature with a 20X 0.40 NA Plan Fluor objective on the brightfield channel.

S6. Turbidity Assays

Stock solutions of PA, ELP-PA, and oppositely charged polyelectrolytes (PDMAEMA, 10 kDa, Sigma Aldrich #909866; qP4VP, 28 kDa, Polymer Source #P-1548-4VPQ; and PAH 17.5 kDa, Sigma Aldrich #283215-5G) were made in 10 mM tris, pH 7.4 and filtered using a 0.22 µm PES Thermo Scientific Nalgene 25 mm Syringe Filter. Stock solution concentrations were 0.8 mg/mL for all ELP-PA turbidity assays and 1 mg/mL for all PA homopeptide turbidity assays. Mixing ratios were selected based on the fraction of positive charge out of total charge present in the sample. Charge fraction was calculated based on the following equation: $f^+ = \frac{c_+ * m_+}{c_+ * m_+ + c_- * m_-}$, where f^+ is positive charge fraction, $c_{+/-}$ is the charge per gram of protein and $m_{+/-}$ is the mass of polyelectrolyte present in

the sample. Charge per gram of protein was calculated using the molecular weight of the protein and the charge state of the constituent amino acids at a pH of 7.4, estimated using the Henderson-Hasselbach equation and the pK_a of each charged amino acid. Initial turbidity assays of PA WT with PDMAEMA, qP4VP, PAH, and GFP(+36) at room temperature were performed in triplicate. All subsequent turbidity assays, including temperature ramp assays and salt titrations with PA polyanions and ELP-PA fusions were performed in duplicate. All turbidity assays were performed on a non-tissue culture treated polystyrene 96-well half-area plate with a low evaporation lid (Corning, Ref #3884), with each well containing a total sample volume of 50 µL. The absorbance at 750 nm was measured in each well on a plate reader (Tecan Infinite M200 Pro). This absorbance was then converted to turbidity using the following formula: turbidity = $100 - 10^{2-A}$.

To prepare samples at specific salt concentrations, the requisite amount of 5 M NaCl solution was added to each well of the 96-well plate (0-4 µL). The plate was then incubated at 37 °C for 1 h to remove the water via evaporation, leaving the correct weight of crystallized NaCl in each well. This NaCl redissolved, upon addition of the PA and oppositely charged polyelectrolyte solutions. To perform temperature ramp turbidity assays, samples were prepared on ice and then incubated at 5 °C in a MaxQ™ 6000 Incubated/Refrigerated Stackable Shaker (Fisher Scientific) for 20 min. After 20 min, absorbance measurements were measured as previously described and the setpoint of the incubator was increased 5 °C. This process was repeated up to a temperature of 60 °C.

S7. Data Processing and Generation of Heatmaps

To process turbidity assay data, absorbance values were imported into Microsoft Excel and converted to turbidity values (turbidity = $100 - 10^{2-A}$). The duplicate turbidity values for each salt concentration, temperature, and charge fraction measurement point were averaged. The average turbidity values for each PA variant at the 12 different temperatures were divided into tables, with each measured salt concentration corresponding to a column and each measured charge fraction corresponding to a row. Each data table was saved as its own Excel file. These Excel files were then imported into R by a script, where a heatmap was generated for each PA variant and temperature and exported as an .svg file. For heatmaps shown in the SI, a separate, but similar script was used to generate 12 heat maps for each cell line, each heatmap representing a single temperature. The script then concatenated these heatmaps into a single image that was exported as a .png

S8. Dynamic Light Scattering (DLS)

Dynamic light scattering was performed on a Malvern Zetasizer using 40 µL disposable plastic cuvettes (Malvern, ZEN0040). To the cuvette, a 0.8 mg/mL ELP-PA solution in 10 mM tris at pH 7.4 was added and then mixed with a 0.8 mg/mL GFP(+36) solution in 10

mM tris, pH 7.4. Samples were made to a total volume of 100 µL, with mixing ratios determined by the desired positive charge fraction of the sample. For variable temperature experiments, 50 µL of silicone oil was layered on top of each sample to prevent evaporation. For salt titrations, a 5 M NaCl stock solution was added to the sample and then mixed via vigorous pipetting. The sample was then given 15-20 min to equilibrate, before DLS measurements were taken.

S9. Size Exclusion Chromatography Multi-Angle Light Scattering (SEC-MALS)

SEC-MALS samples were prepared at a total macromolecule concentration of 0.8 mg/mL in 10 mM tris at pH 7.4 at a temperature of 5 °C. Samples were separated via size exclusion chromatography using an Agilent 1260 HPLC system with a Diode-Array detector and a fluorescence detector and a Superdex 200 10/300 GL SEC column (Cytiva, #17517501). MALS data was collected using a Dawn Multi-Angle Light Scattering Detector and refractive index data was collected using a Optilab T-rEX refractive index detector. MALS data was fit using a Debye light scattering model, assuming a $\frac{d_n}{d_c}$ of 0.1850 mL/g.[3]

S10. Transmission Electron Microscopy (TEM)

TEM samples were prepared by mixing the ELP-PA variant and GFP(+36) at the positive charge fraction that corresponded to the preferred micellar composition ($f^+ = 0.6$) in 10 mM tris buffer at pH 7.4 with a 0.8 mg/mL total macromolecule concentration. In some cases, this sample was diluted 10-fold in ddH_2O prior to spotting. 5 µL of the diluted sample was spotted at 5 °C onto a Formvar coated, 300 mesh, copper grid (Ted Pella 01701-F). The sample was immediately wicked with filter paper to remove excess sample. The spotted grid was then left to dry at 5 °C for 4-6 h and then transferred to a desiccator at room temperature, where residual water was removed under low pressure for an additional 6-12 h. TEM was then performed using an EI Talos F200X Transmission / Scanning Electron Microscope (S/TEM) in TEM mode.

S11. Figure S1. Electrophoresis analysis of engineered PA Proteins

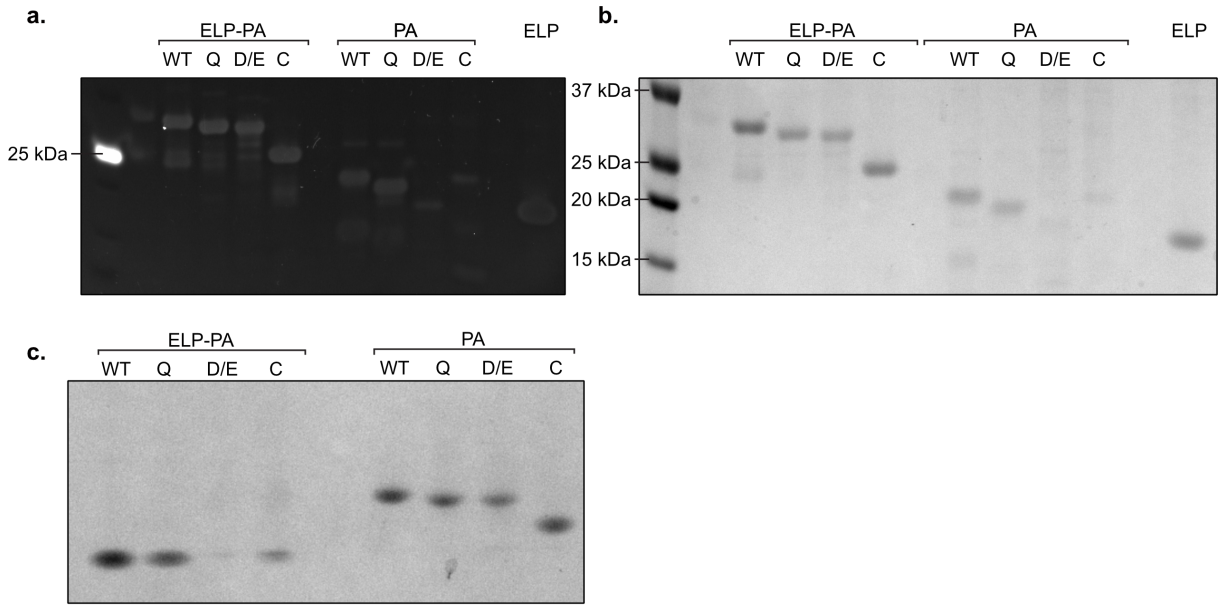

Figure S1. SDS-PAGE (a, b) analysis of PA polyanions and ELP fusions, stained with polyhistidine stain (a) and Coomassie stain (b). (c) Native-PAGE analysis of PA polyanions and ELP fusions, stained with Coomassie stain. Samples were run at a concentration of 0.04 mg/mL.

S12. Figure S2. Cloud point determination of elastin-like peptides

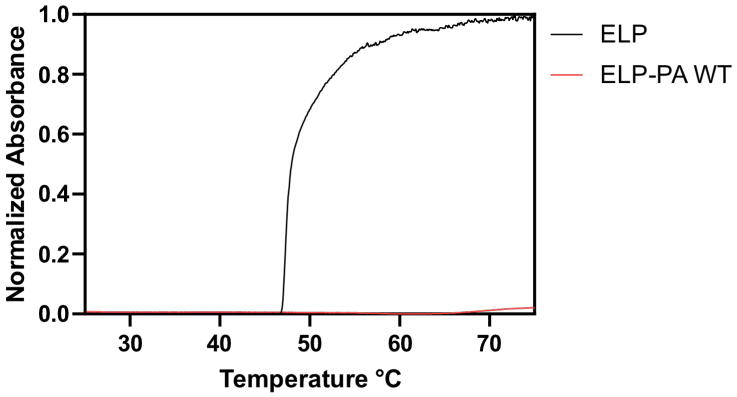

Figure S2. Cloud point measurements for ELP peptide and ELP-PA WT fusion proteins. Proteins were prepared at a concentration of 0.8 mg/mL in 10 mM tris at pH 7.4. Absorbance was measured at a wavelength of 600 nm and temperature was increased at a rate of 0.5 °C / min.

S13. Figure S3. Light microscopy of PA or ELP-PA variants and GFP(+36)

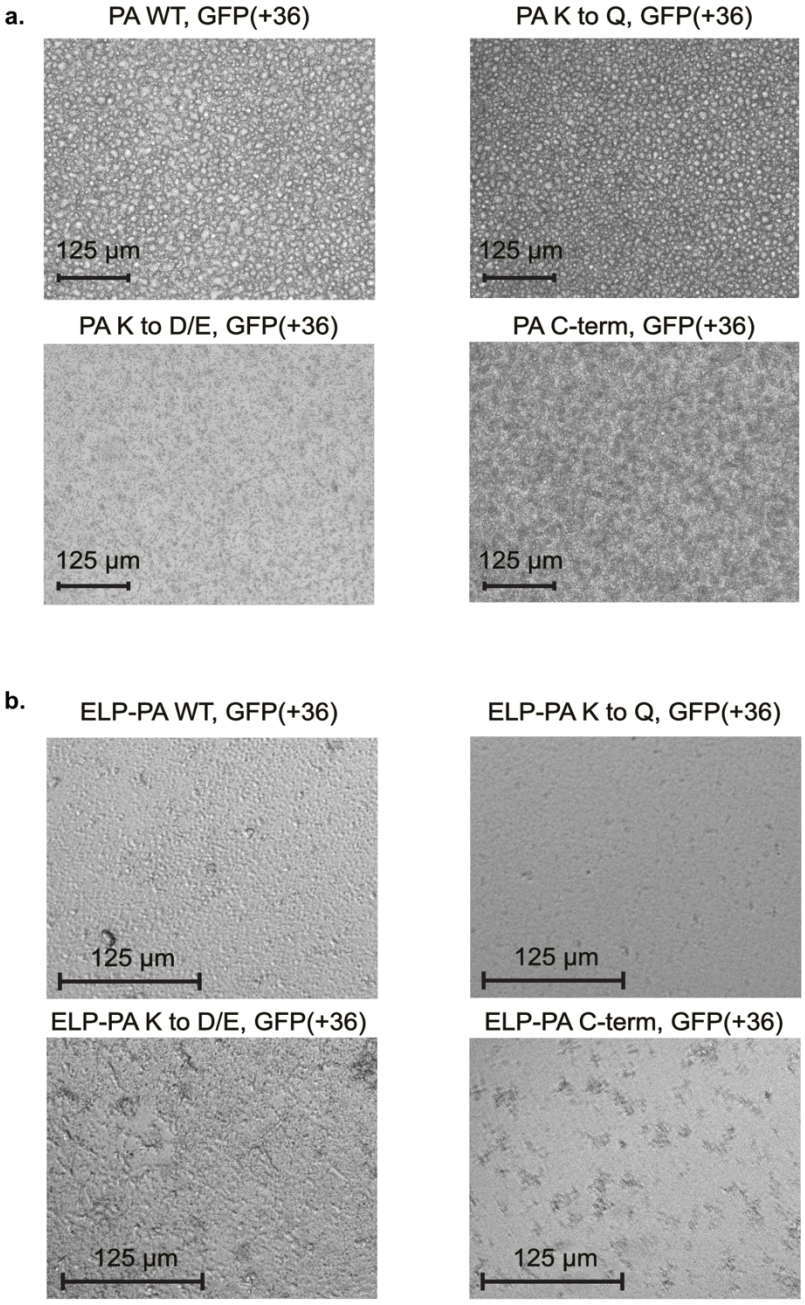

Figure S3. (a) Light microscopy images of PA polyanions mixed with GFP(+36) at a total macromolecule concentration of 1 mg/mL and $f^+ = 0.5$. (b) Light microscopy images of ELP-PA block copolymers mixed with GFP(+36) at a total macromolecule concentration of 0.8 mg/mL and $f^+ = 0.6$. Samples were prepared in 10 mM tris buffer at pH 7.4 and were incubated in the plate for at least 1 h prior to imaging. Images were taken using a 20x objective, scale bar 125 µm.

Figure S4. DLS results of ELP-PA and GFP(+36) mixtures at 5 °C

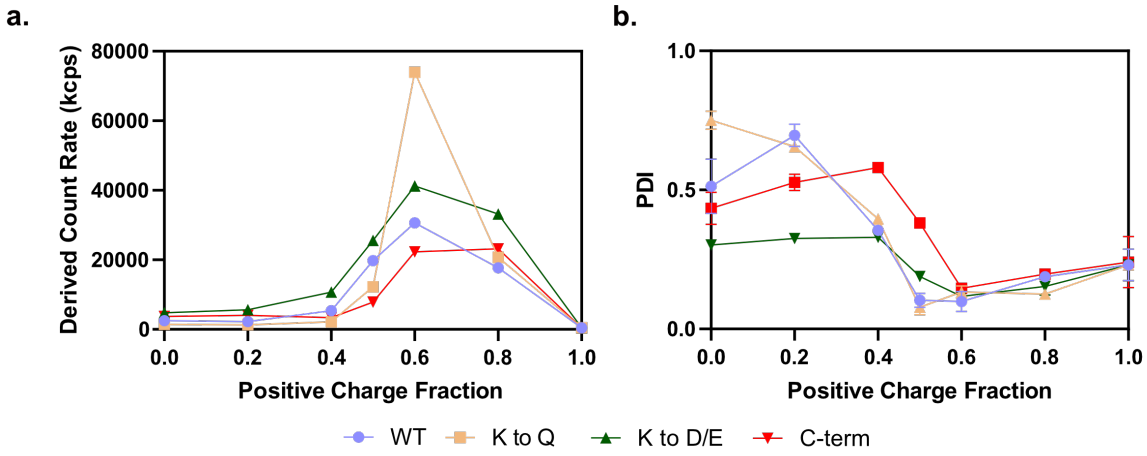

Figure S4. DLS results of ELP-PA fusions mixed with GFP(+36) at varying mixing ratios at a total macromolecule concentration of 0.8 mg/mL and a temperature of 5 °C. (a) Derived count rate and (b) Polydispersity index (PDI) indicate polyelectrolyte complex formation between positive charge fractions of 0.5 and 0.8.

Figure S5. SEC-MALS data for ELP-PA WT mixed with GFP(+36)

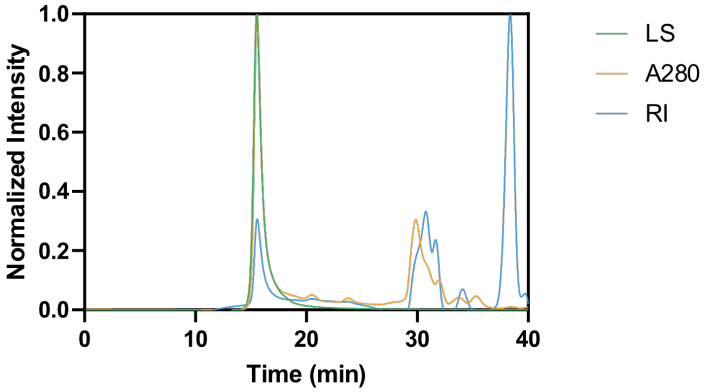

Figure S5. SEC-MALS results of ELP-PA WT mixed with GFP(+36) at 0.6 positive charge fraction, with a total macromolecule concentration of 0.8 mg/mL. Samples were analyzed at a temperature of 5 °C. Traces shown include light scattering (LS), absorbance (A280, λ = 280 nm), and refractive index (RI).

S14. Figure S6. DLS correlation functions for ELP-PA / GFP(+36) mixtures at 5 °C

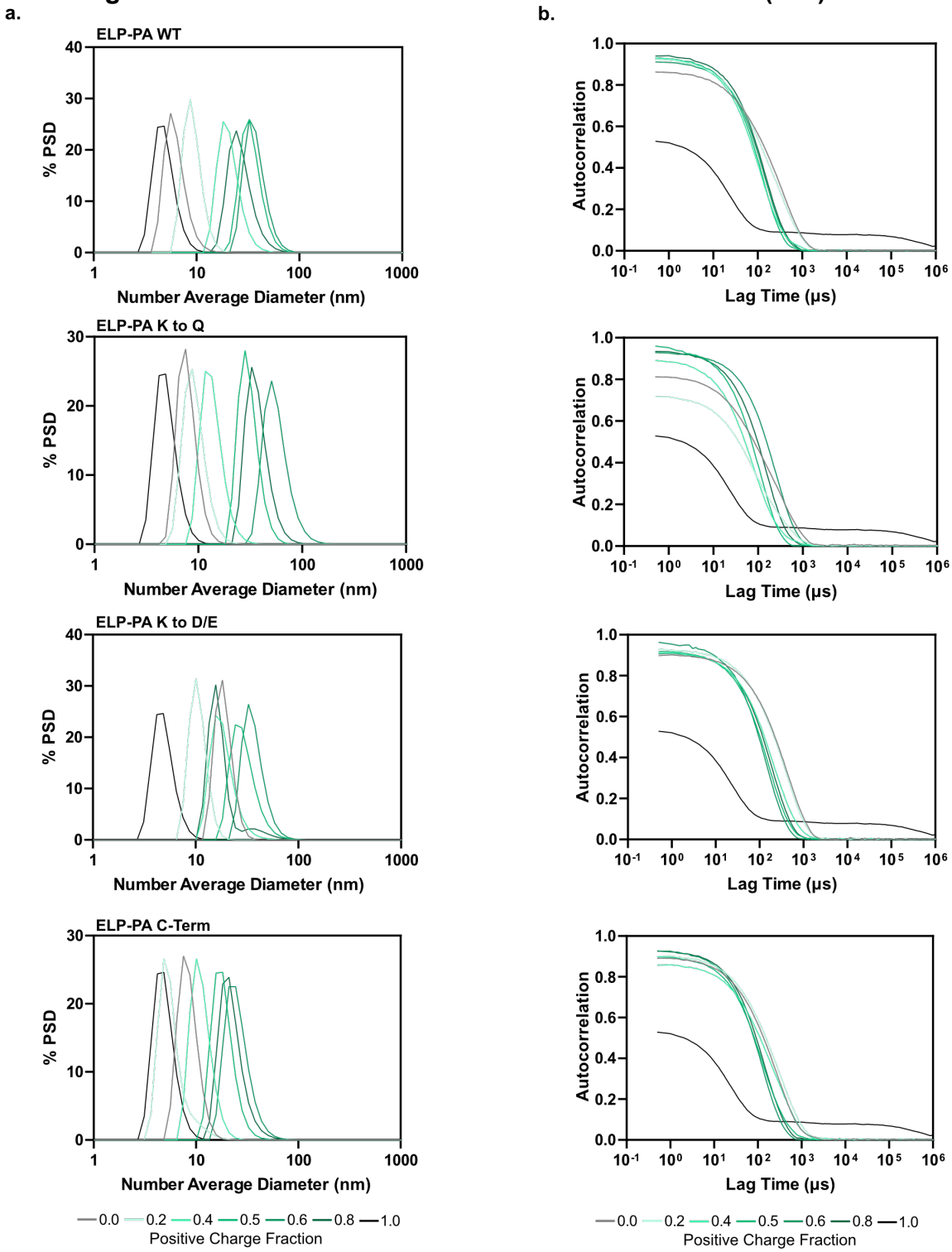

Figure S6. Number average particle size distributions (a) and autocorrelation functions (b) for ELP-PA variants mixed with GFP(+36) at 0 mM NaCl in 10 mM tris (pH 7.4) at 5 °C.

S15. Figure S7. Turbidity assays for PA WT as a function of temperature

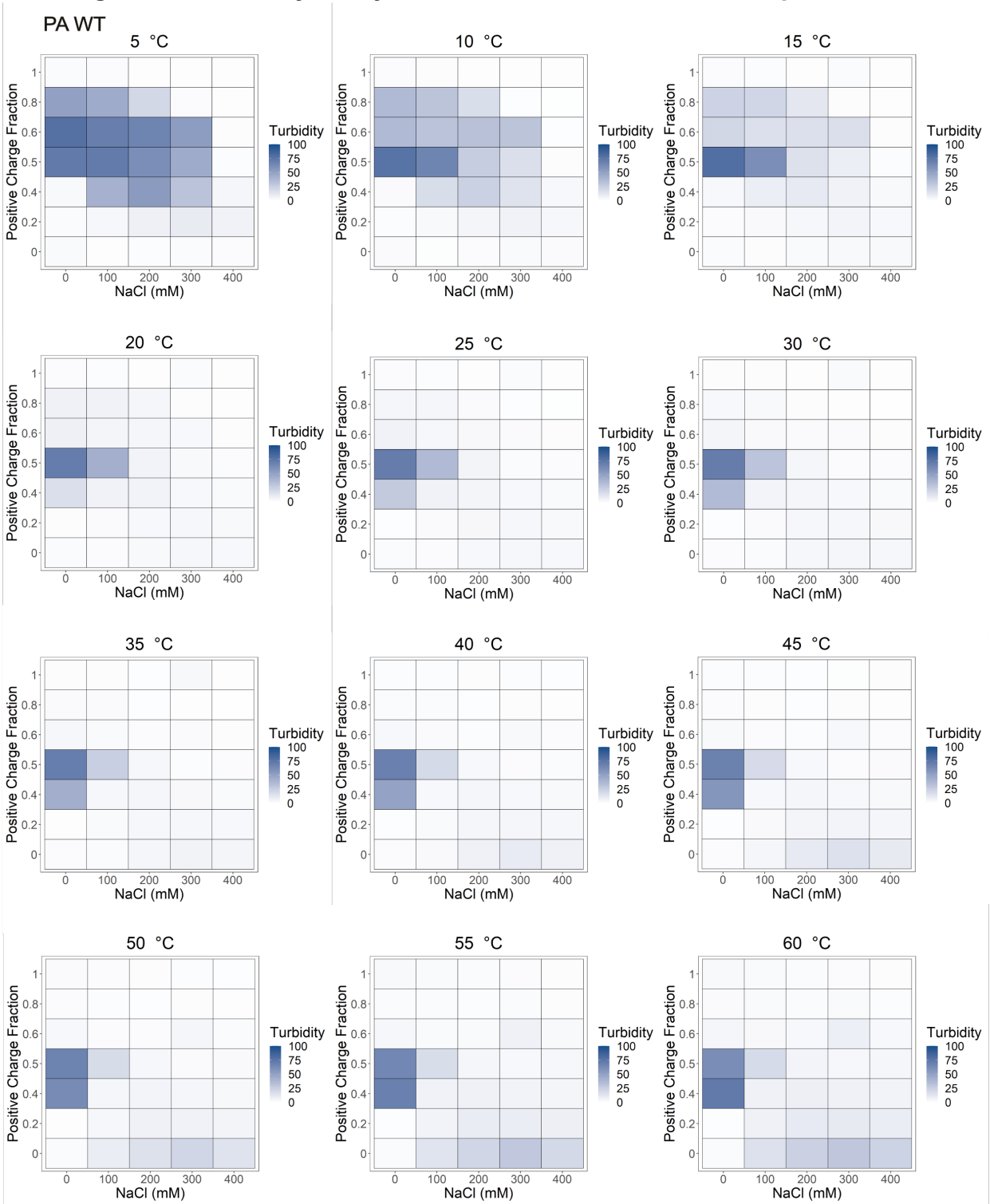

Figure S7. Full temperature-dependent turbidity assays for PA WT mixed with GFP(+36). Samples were mixed at a total macromolecule concentration of 1.0 mg/mL in 10 mM tris at pH 7.4 and varying concentrations of NaCl, as indicated.

S16. Figure S8. Turbidity assays for PA K to Q as a function of temperature

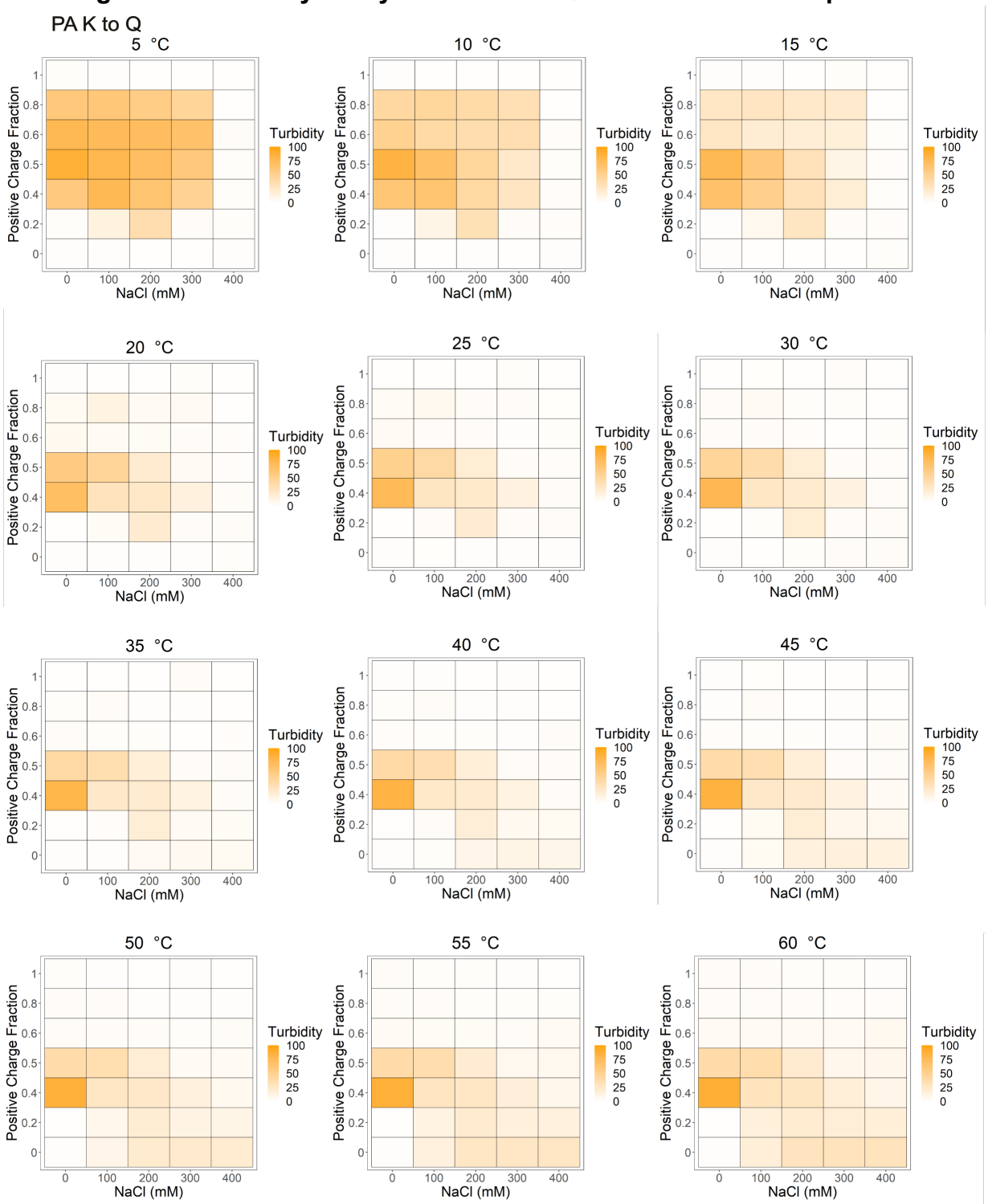

Figure S8. Full temperature-dependent turbidity assays for PA K to Q mixed with GFP(+36). Samples were mixed at a total macromolecule concentration of 1.0 mg/mL in 10 mM tris at pH 7.4 and varying concentrations of NaCl, as indicated.

S17. Figure S9. Turbidity assays for PA K to D/E as a function of temperature

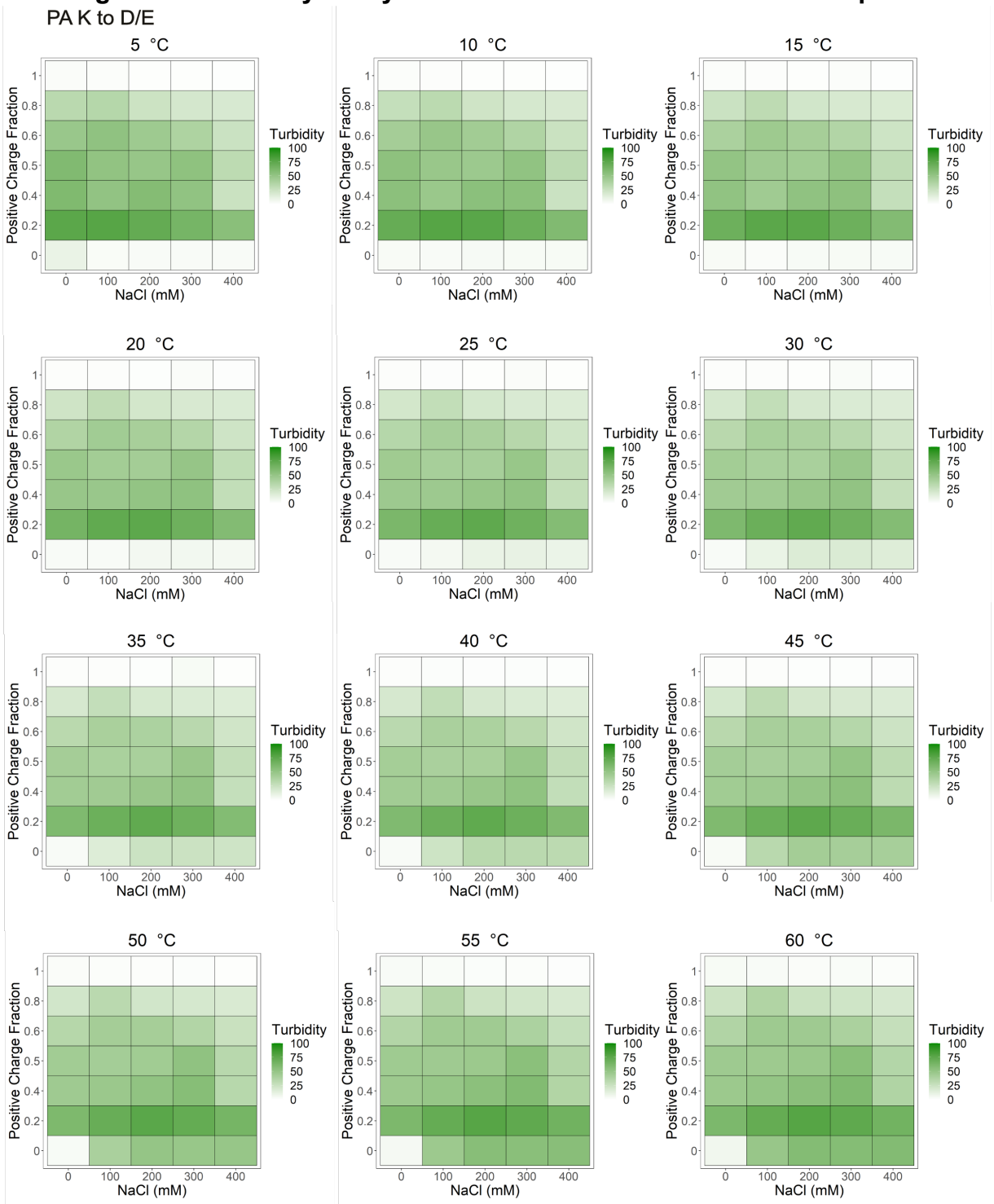

Figure S9. Full temperature-dependent turbidity assays for PA K to D/E mixed with GFP(+36). Samples were mixed at a total macromolecule concentration of 1.0 mg/mL in 10 mM tris at pH 7.4 and varying concentrations of NaCl, as indicated.

S18. Figure S10. Turbidity assays for PA C-term as a function of temperature

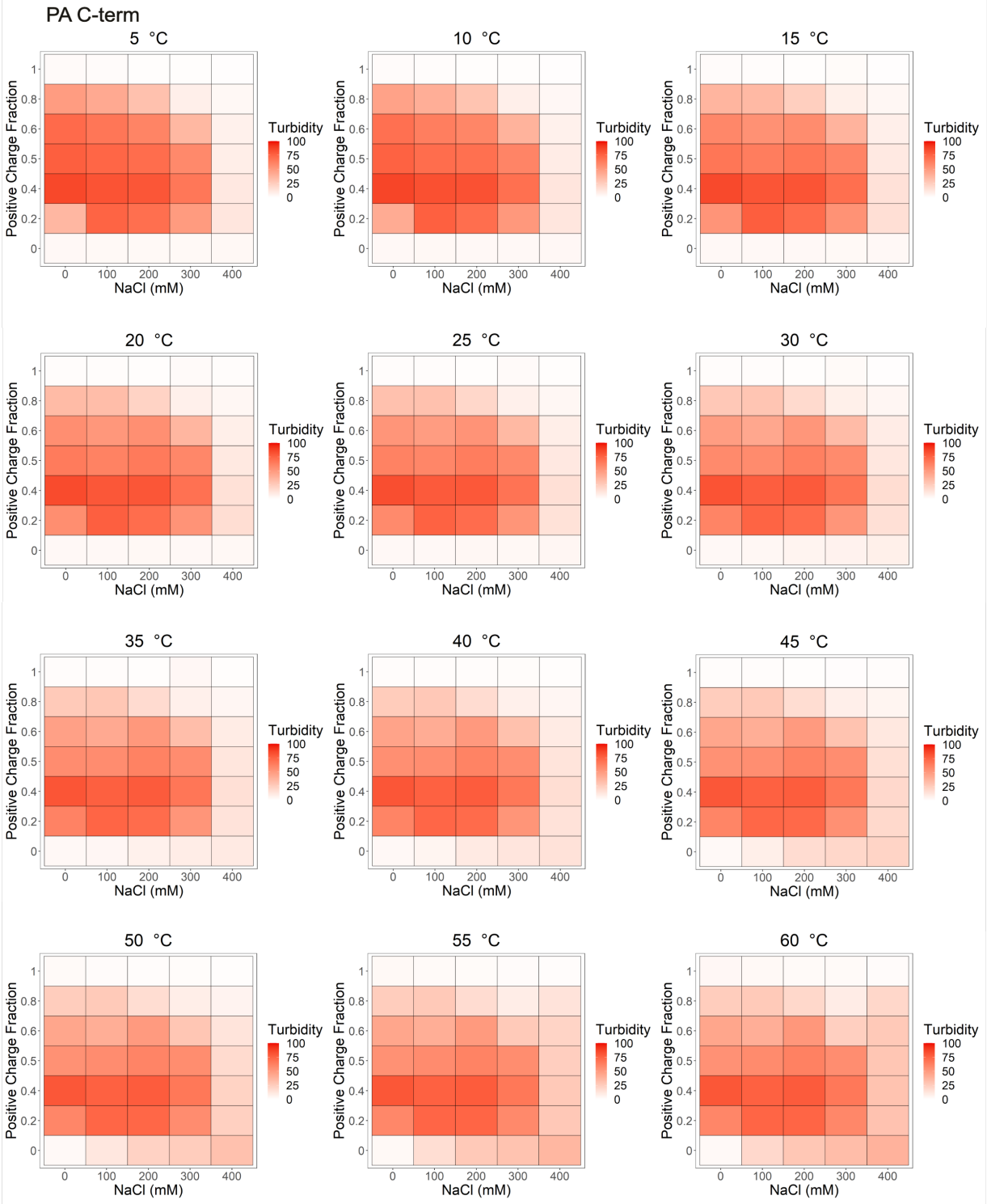

Figure S10. Full temperature-dependent turbidity assays for PA C-term mixed with GFP(+36). Samples were mixed at a total macromolecule concentration of 1.0 mg/mL in 10 mM tris at pH 7.4 and varying concentrations of NaCl, as indicated.

S19. Figure S11. Turbidity assays for ELP-PA WT as a function of temperature

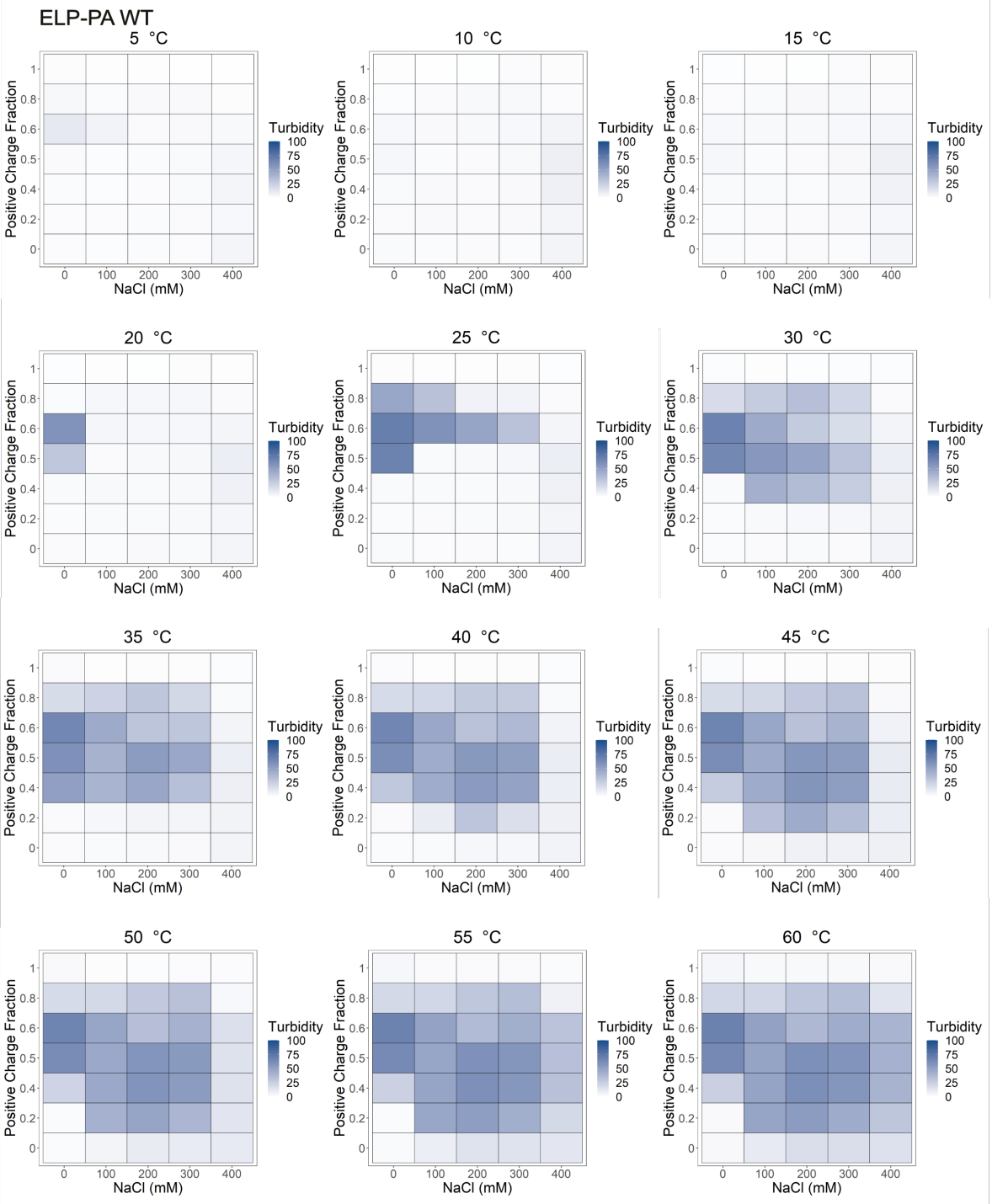

Figure S11. Full temperature-dependent turbidity assays for ELP-PA WT mixed with GFP(+36). Samples were mixed at a total macromolecule concentration of 0.8 mg/mL in 10 mM tris at pH 7.4 and varying concentrations of NaCl, as indicated.

S20. Figure S12. Turbidity assays for ELP-PA K to Q as a function of temperature

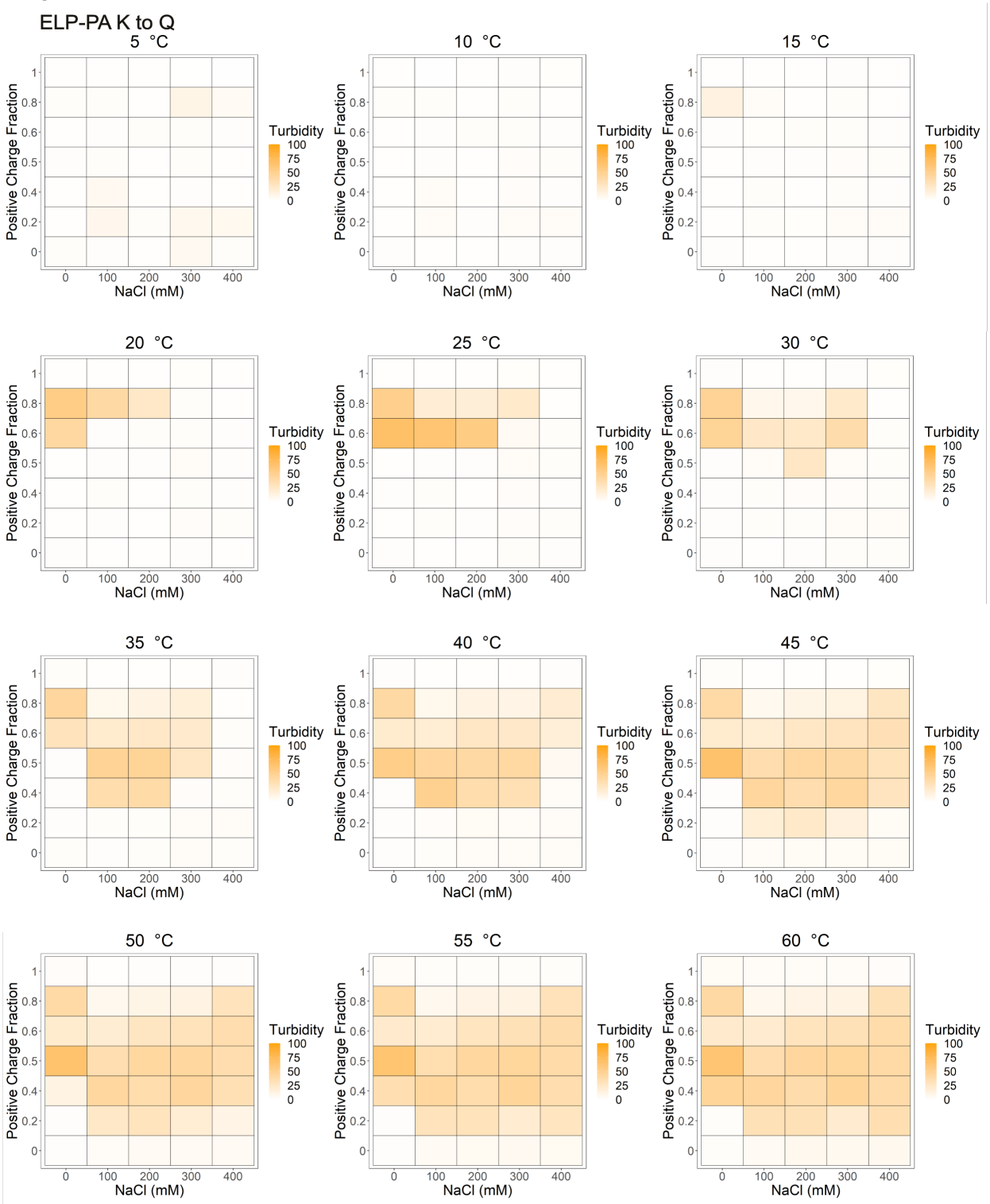

Figure S12. Full temperature-dependent turbidity assays for ELP-PA K to Q mixed with GFP(+36). Samples were mixed at a total macromolecule concentration of 0.8 mg/mL in 10 mM tris at pH 7.4 and varying concentrations of NaCl, as indicated.

S21. Figure S13. Turbidity assays for ELP-PA K to D/E as a function of temperature

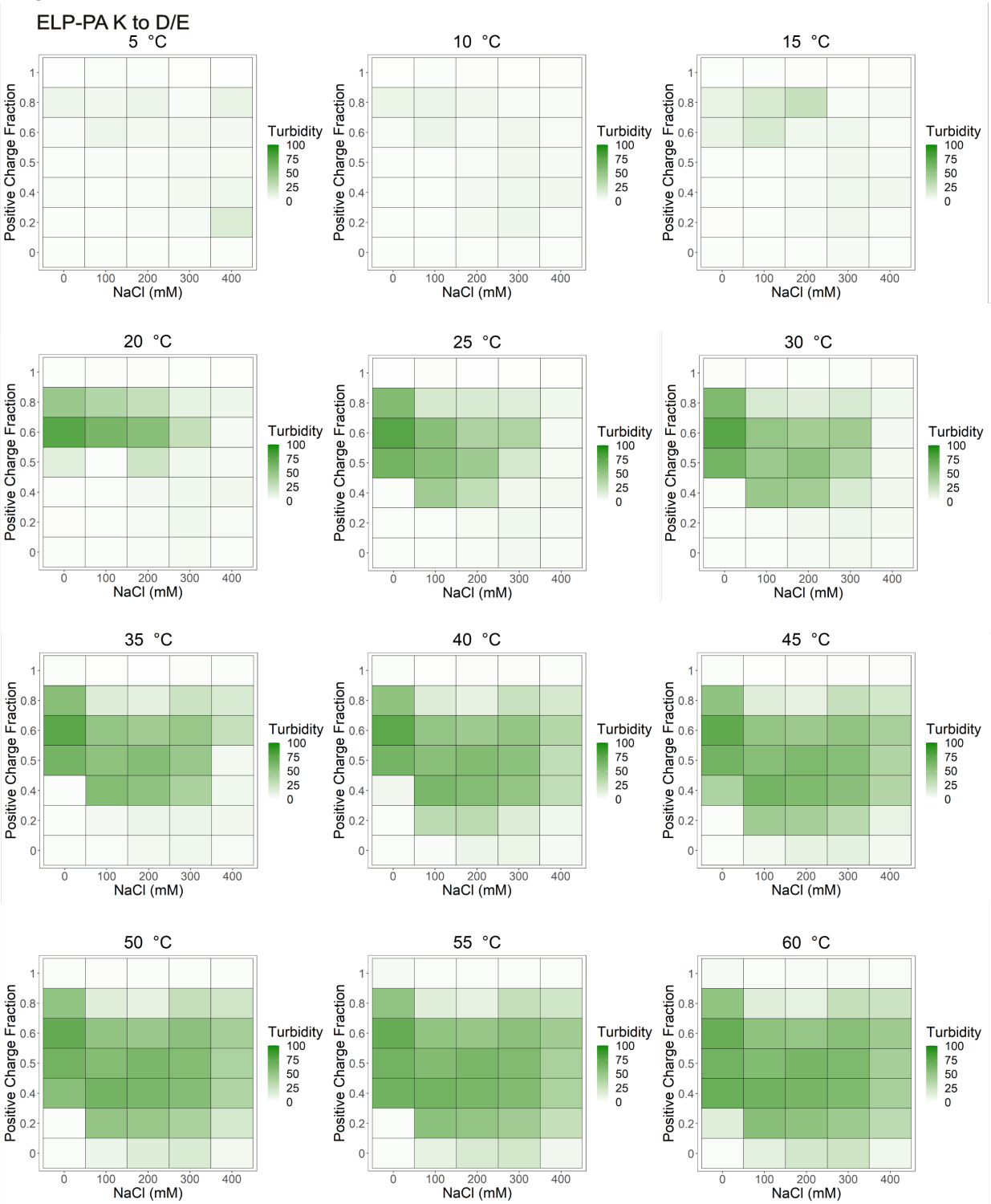

Figure S13. Full temperature-dependent turbidity assays for ELP-PA K to D/E mixed with GFP(+36). Samples were mixed at a total macromolecule concentration of 0.8 mg/mL in 10 mM tris at pH 7.4 and varying concentrations of NaCl, as indicated.

S22. Figure S14. Turbidity assays for ELP-PA C-term as a function of temperature

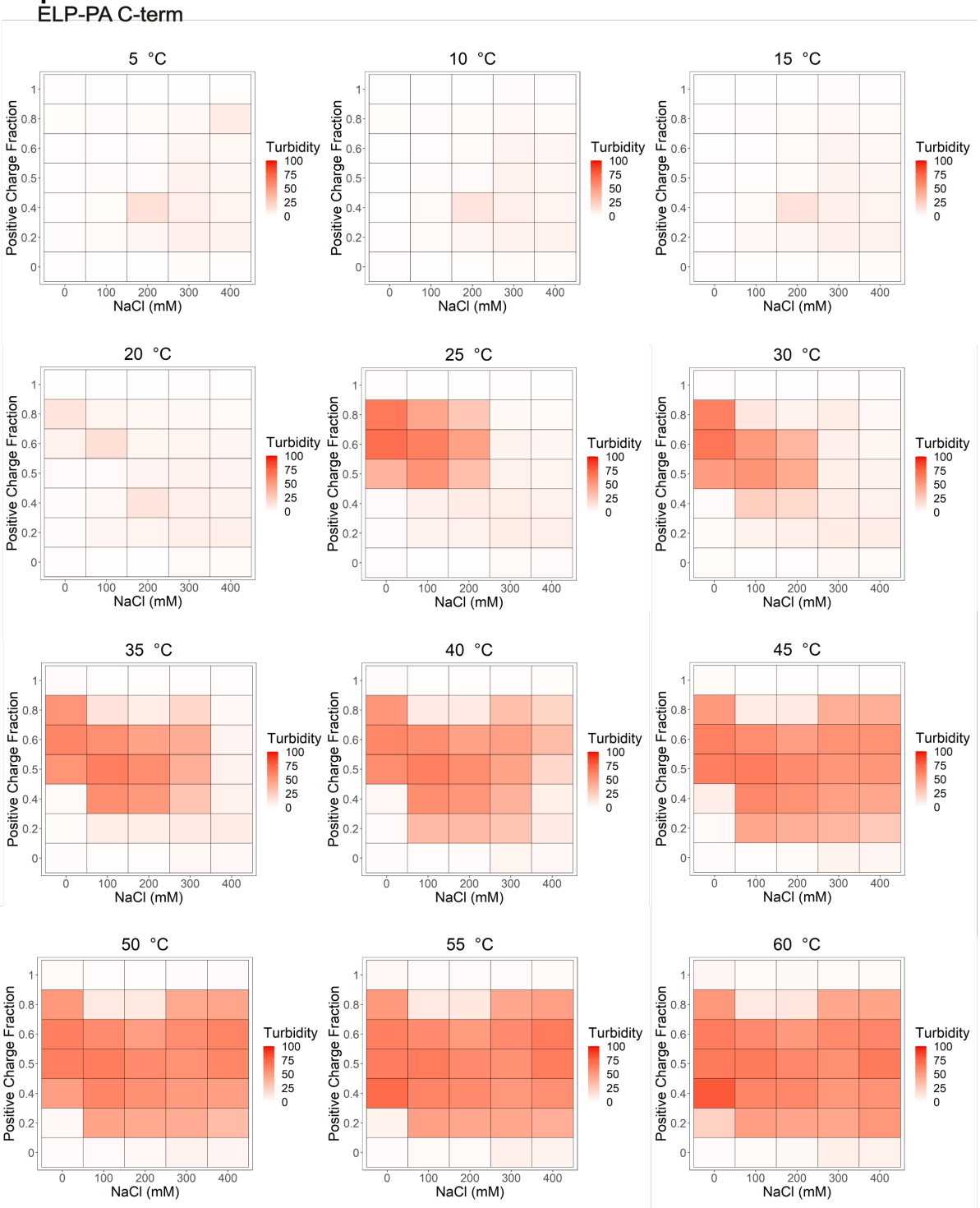

Figure S14. Full temperature-dependent turbidity assays for ELP-PA C-term mixed with GFP(+36). Samples were mixed at a total macromolecule concentration of 0.8 mg/mL in 10 mM tris at pH 7.4 and varying concentrations of NaCl, as indicated.

S23. Figure S15. DLS correlation functions as a function of salt concentration for ELP-PA WT / GFP(+36) at 5 °C

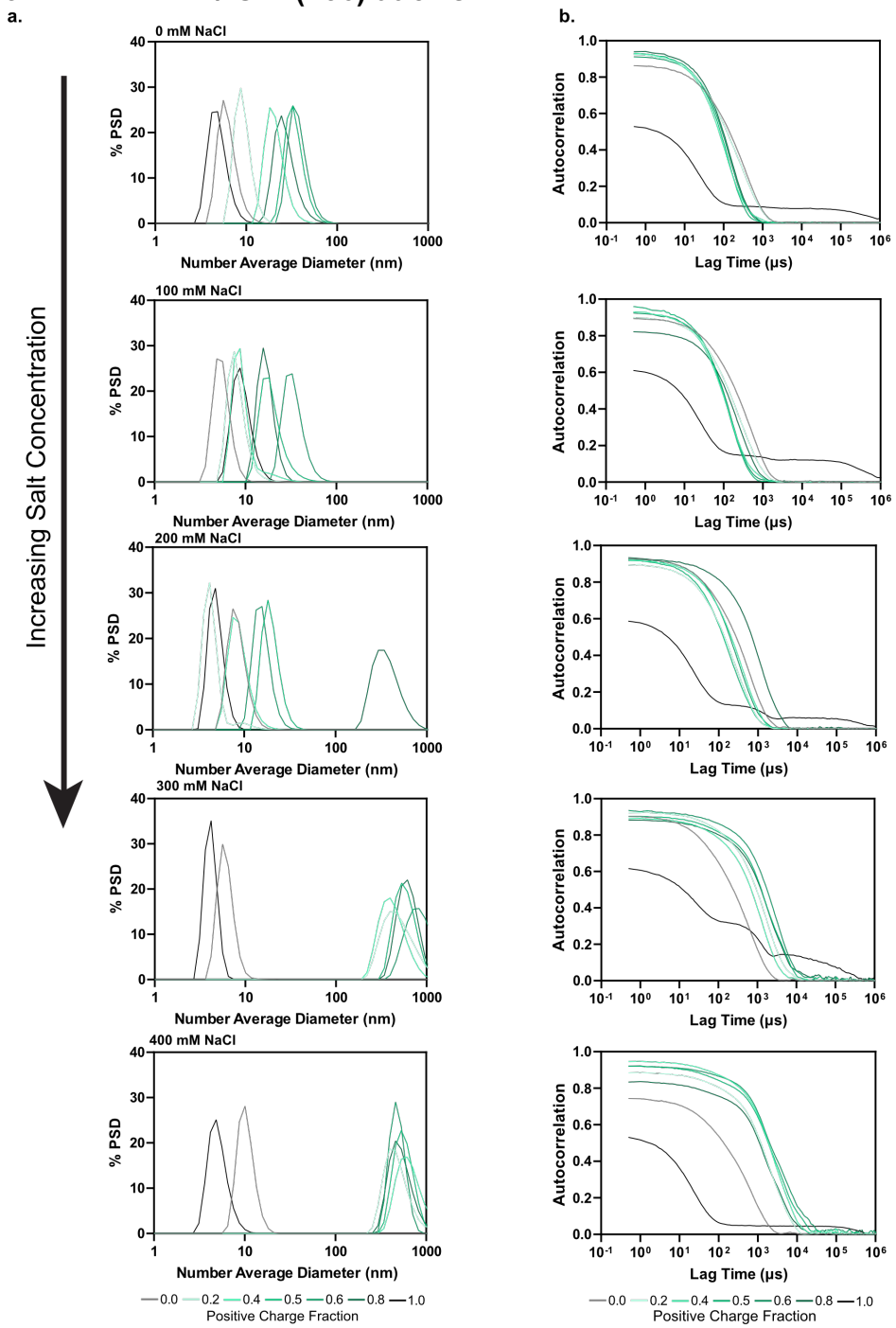

Figure S15. Number average particle size distributions (a) and autocorrelation functions (b) for ELP-PA WT mixed with GFP(+36) at a total macromolecule concentration of 0.8 mg/mL and 5 °C and varying salt concentrations. Data for 0 mM NaCl is also shown in Figure S6.

S24. Figure S16. DLS correlation functions as a function of salt concentration for ELP-PA K to Q / GFP(+36) at 5 °C

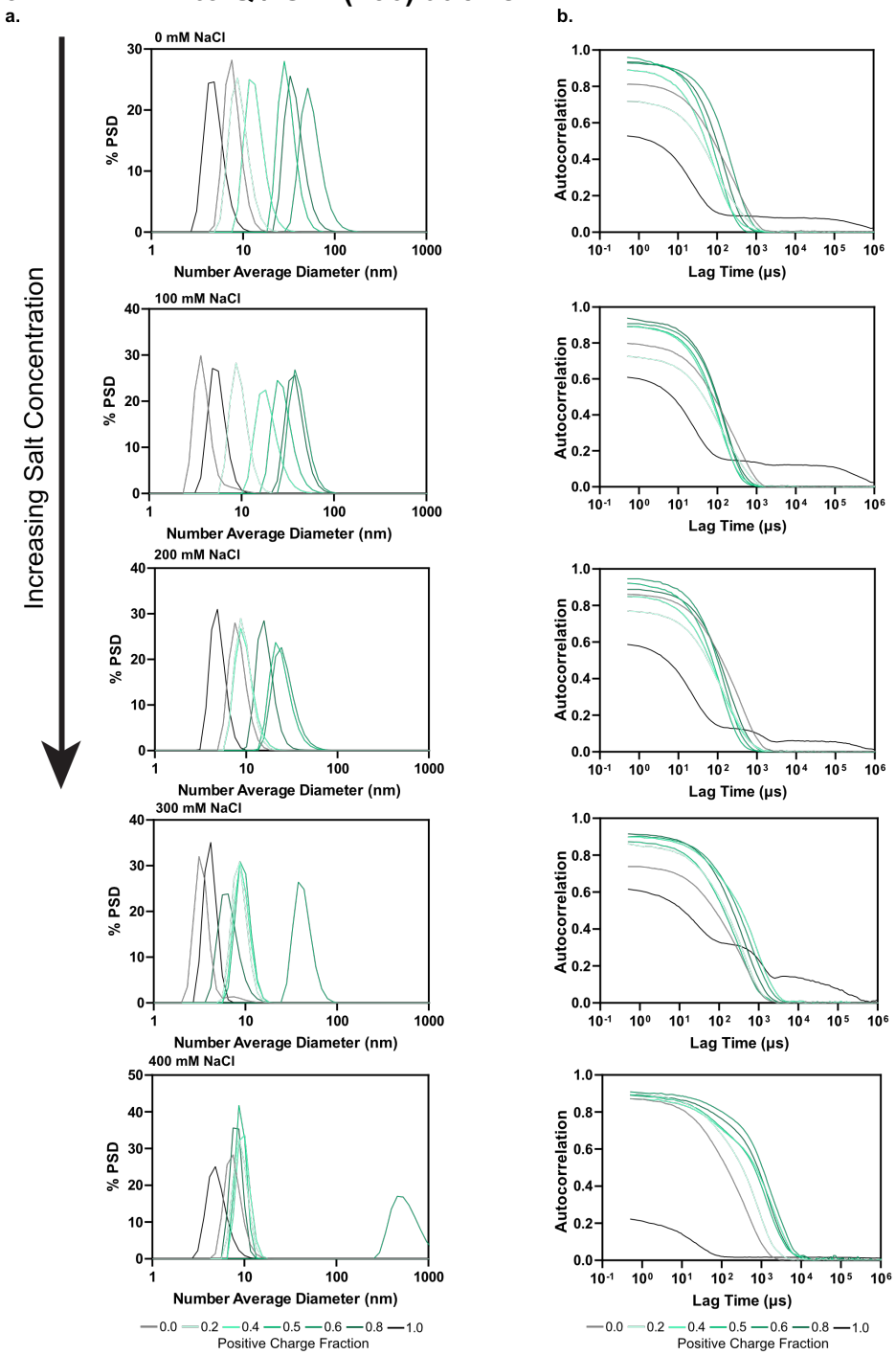

Figure S16. Number average particle size distributions (a) and autocorrelation functions (b) for ELP-PA K to Q mixed with GFP(+36) at a total macromolecule concentration of 0.8 mg/mL and 5 °C and varying salt concentrations. Data for 0 mM NaCl is also shown in Figure S6.

S25. Figure S17. DLS correlation functions as a function of salt concentration for ELP-PA K to D/E / GFP(+36) at 5 °C

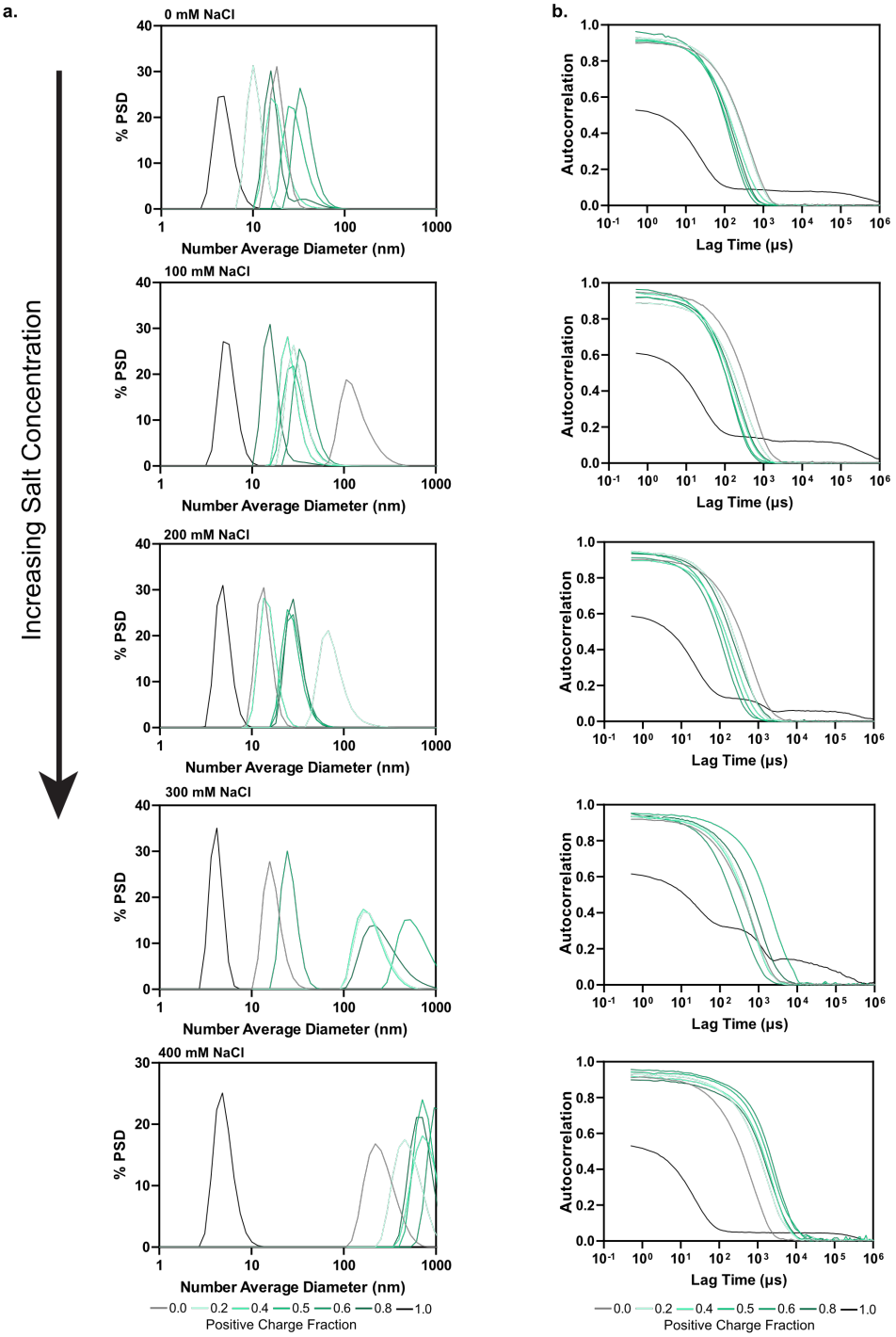

Figure S17. Number average particle size distributions (a) and autocorrelation functions (b) for ELP-PA K to D/E mixed with GFP(+36) at a total macromolecule concentration of 0.8 mg/mL and 5 °C and varying salt concentrations. Data for 0 mM NaCl is also shown in Figure S6.

S26. Figure S18. DLS correlation functions as a function of salt concentration for ELP-PA C-term / GFP(+36) at 5 °C

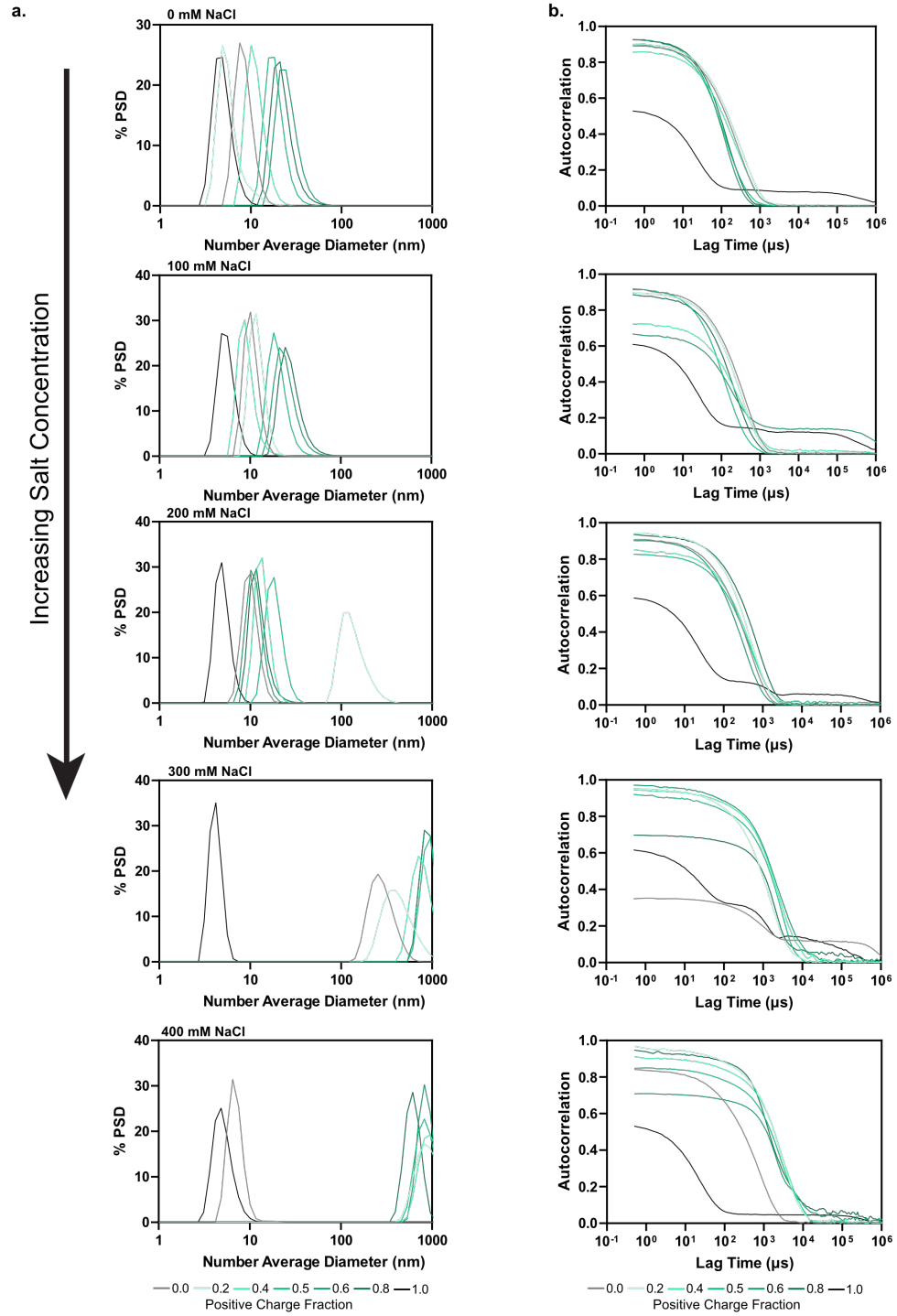

Figure S18. Number average particle size distributions (a) and autocorrelation functions (b) for ELP-PA C-term mixed with GFP(+36) at a total macromolecule concentration of 0.8 mg/mL and 5 °C and varying salt concentrations. Data for 0 mM NaCl is also shown in Figure S6.

S27. Figure S19. DLS data for ELP-PA WT / GFP(+36) at 5 °C as a function of salt concentration

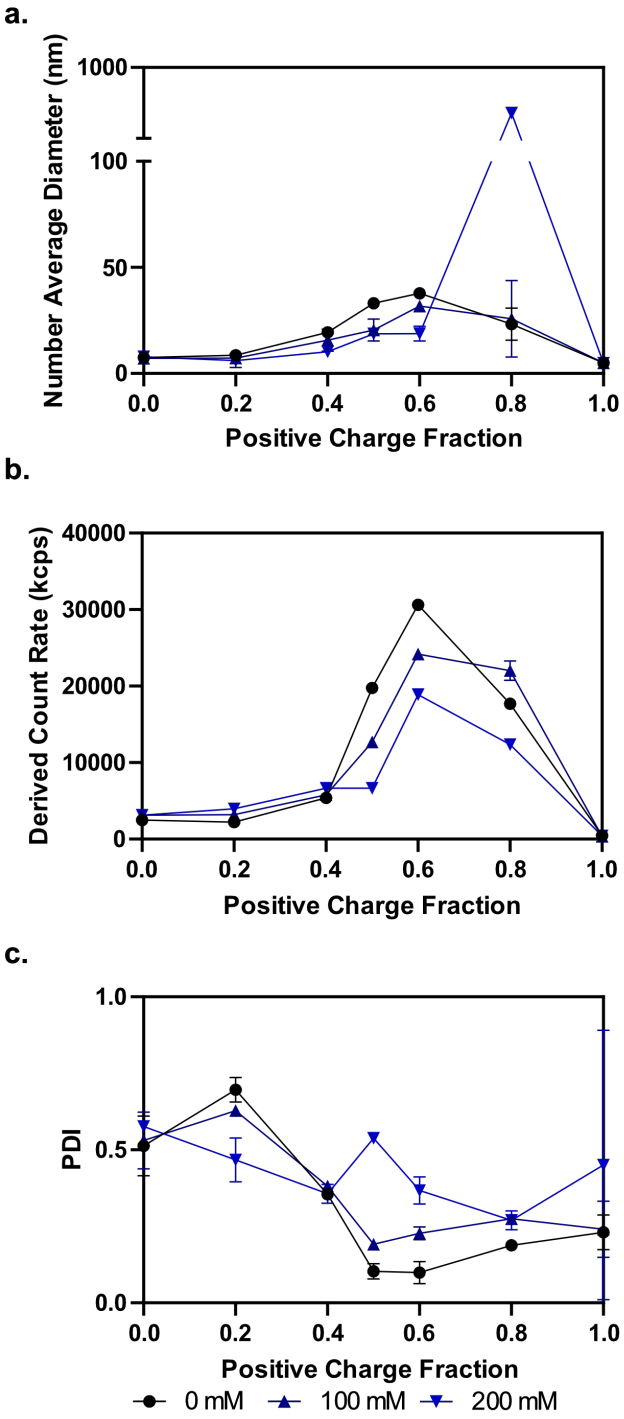

Figure S19. Number average diameter (a), derived count rate (b), and PDI (c) of ELP-PA WT mixed with GFP(+36) at a total macromolecule concentration of 0.8 mg/mL. Samples were made without any NaCl in 10 mM tris at pH 7.4 and NaCl was titrated in by addition of 5 M NaCl solution. Titration increased sample volume by 4% per 100 mM of NaCl added to solution. At the highest NaCl concentration (400 mM), the total macromolecule concentration was decreased to 0.69 mg/mL.

S28. Figure S20. DLS data for ELP-PA K to Q / GFP(+36) at 5 °C as a function of salt concentration

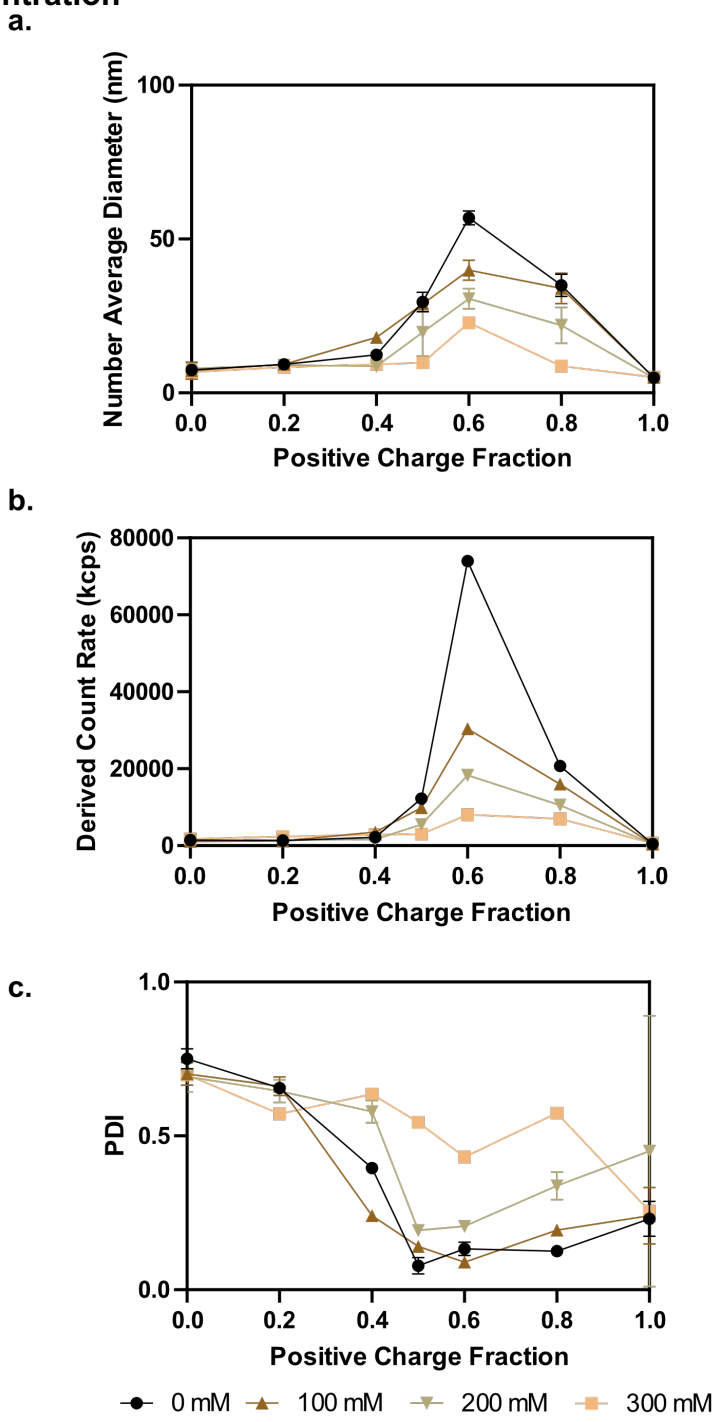

Figure S20. Number average diameter (a), derived count rate (b), and PDI (c) of ELP-PA K to Q mixed with GFP(+36) at a total macromolecule concentration of 0.8 mg/mL. Samples were made without any NaCl in 10 mM tris at pH 7.4 and NaCl was titrated in by addition of 5 M NaCl solution. Titration increased sample volume by 4% per 100 mM of NaCl added to solution. At the highest NaCl concentration (400 mM), the total macromolecule concentration was decreased to 0.69 mg/mL.

S29. Figure S21. DLS data for ELP-PA K to D/E / GFP(+36) at 5 °C as a function of salt concentration

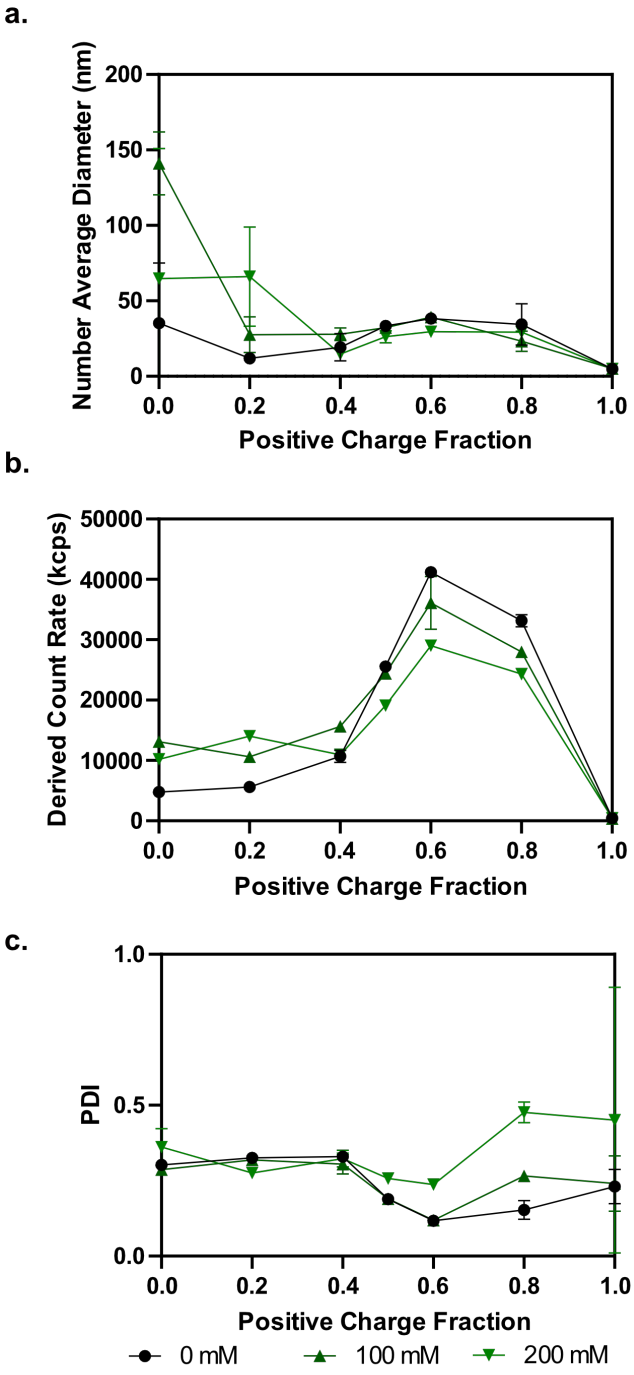

Figure S21. Number average diameter (a), derived count rate (b), and PDI (c) of ELP-PA K to D/E mixed with GFP(+36) at a total macromolecule concentration of 0.8 mg/mL. Samples were made without any NaCl in 10 mM tris at pH 7.4 and NaCl was titrated in by addition of 5 M NaCl solution. Titration increased sample volume by 4% per 100 mM of NaCl added to solution. At the highest NaCl concentration (400 mM), the total macromolecule concentration was decreased to 0.69 mg/mL.

S30. Figure S22. DLS data for ELP-PA C-term / GFP(+36) at 5 °C as a function of salt concentration

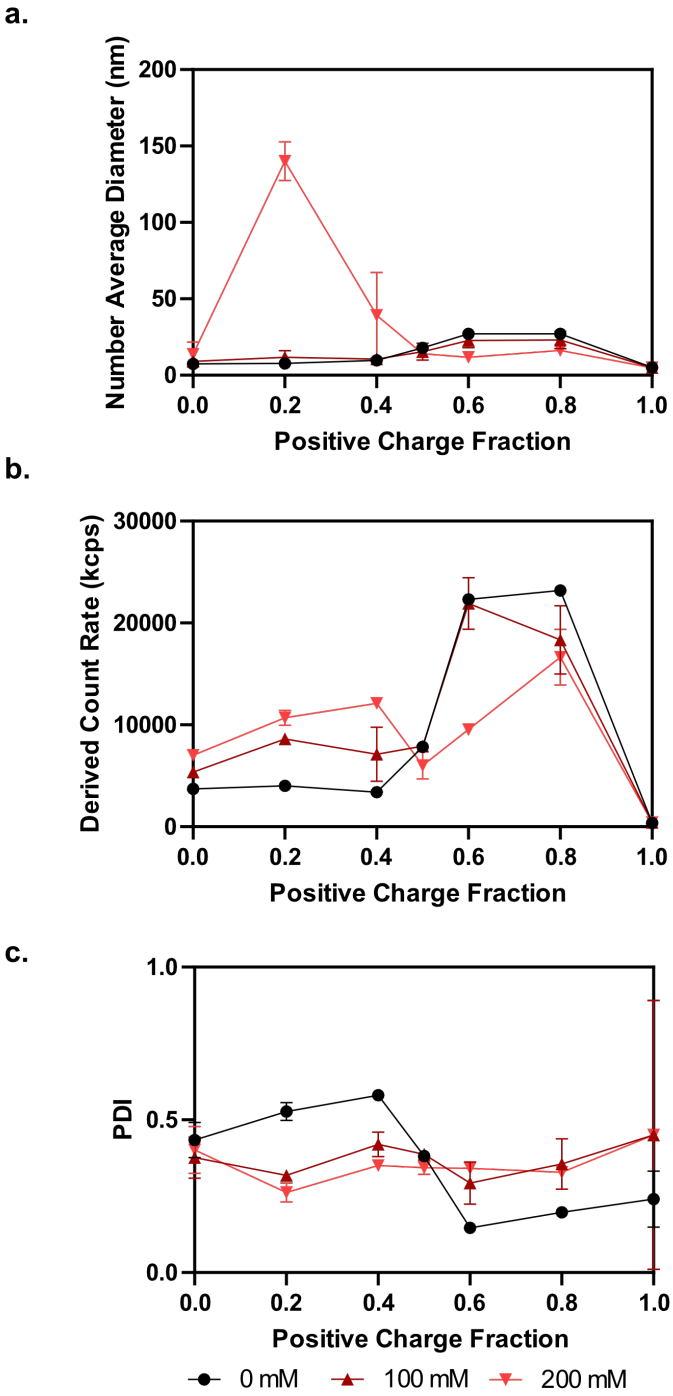

Figure S22. Number average diameter (a), derived count rate (b), and PDI (c) of ELP-PA C-term mixed with GFP(+36) at a total macromolecule concentration of 0.8 mg/mL. Samples were made without any NaCl in 10 mM tris at pH 7.4 and NaCl was titrated in by addition of 5 M NaCl solution. Titration increased sample volume by 4% per 100 mM of NaCl added to solution. At the highest NaCl concentration (400 mM), the total macromolecule concentration was decreased to 0.69 mg/mL.

S31. Figure S23. DLS as a function of temperature for ELP-PA WT / GFP(+36) at $f^+ = 0.6$

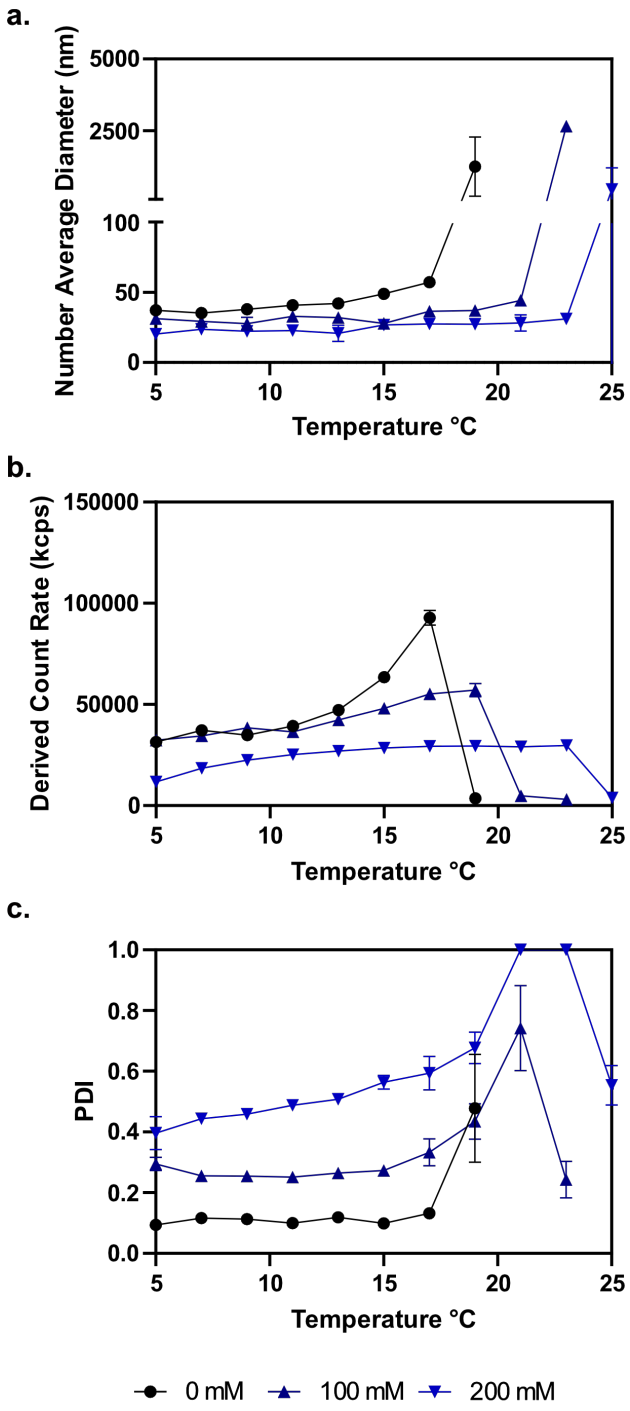

Figure S23. Number average diameter (a), derived count rate (b), and PDI (c) of ELP-PA WT mixed with GFP(+36) at a total macromolecule concentration of 0.8 mg/mL. Samples were made at 5 °C and a positive charge fraction of 0.6 and temperature was increased by 2 °C every 10 min to 35 °C. Data is plotted up to the transition to bulk phase separation. DLS data for bulk phase separation is not shown because DLS is unsuitable for characterizing bulk phase separation due to its dispersity, temporal instability, and inconsistent morphology.

S32. Figure S24. DLS as a function of temperature for ELP-PA K to Q / GFP(+36) at $f^+ = 0.6$

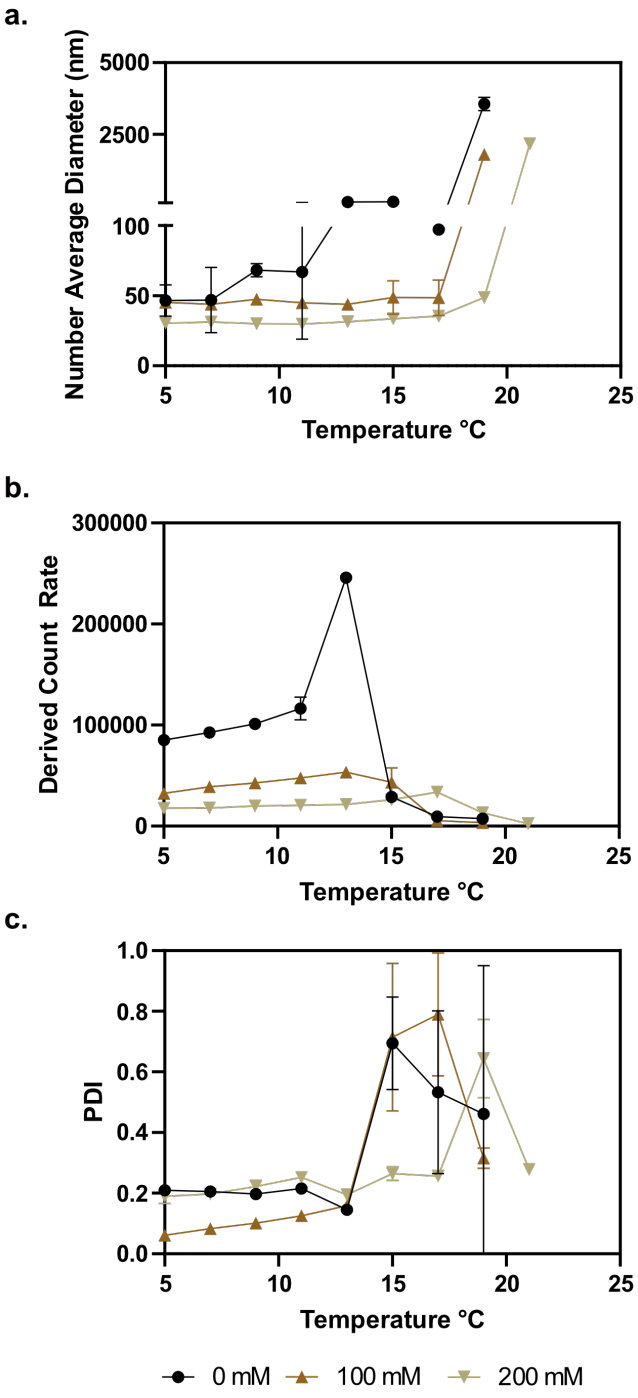

Figure S24. Number average diameter (a), derived count rate (b), and PDI (c) of ELP-PA K to Q mixed with GFP(+36) at a total macromolecule concentration of 0.8 mg/mL. Samples were made at 5 °C and a positive charge fraction of 0.6 and temperature was increased by 2 °C every 10 min to 35 °C. Data is plotted up to the transition to bulk phase separation. DLS data for bulk phase separation is not shown because DLS is unsuitable for characterizing bulk phase separation due to its dispersity, temporal instability, and inconsistent morphology.

S33. Figure S25. DLS as a function of temperature for ELP-PA K to D/E / GFP(+36) at f^+ = 0.6

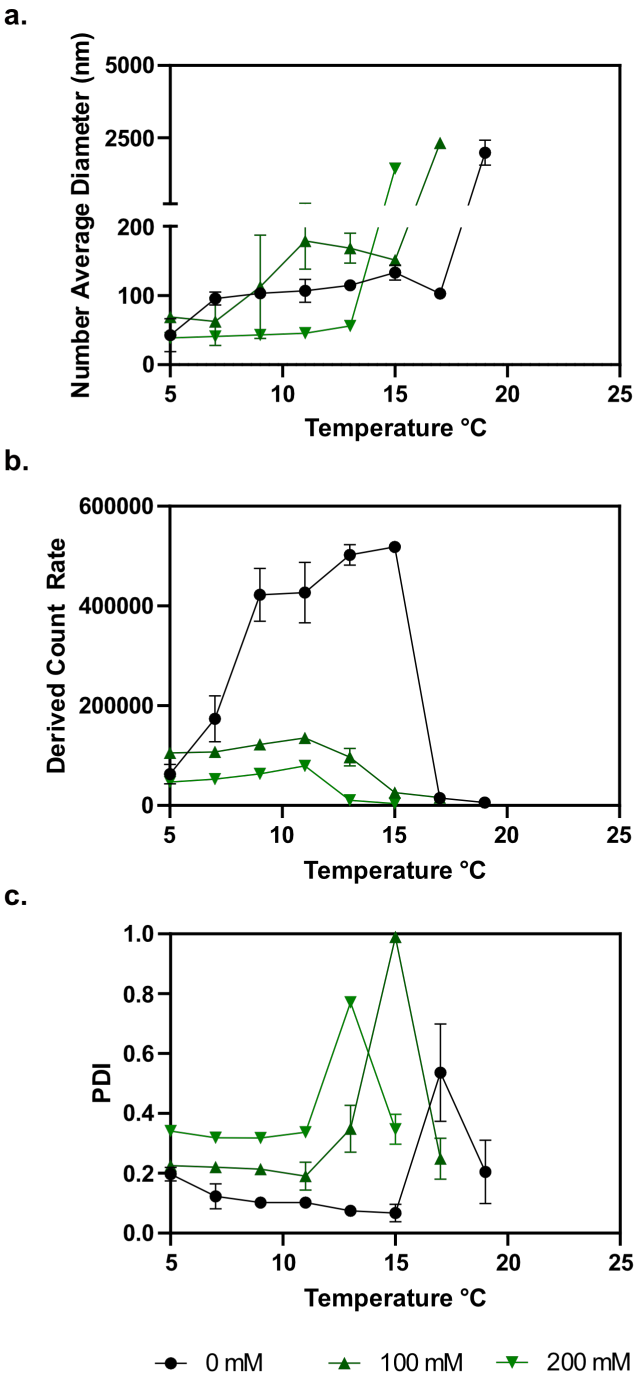

Figure S25. Number average diameter (a), derived count rate (b), and PDI (c) of ELP-PA K to D/E mixed with GFP(+36) at a total macromolecule concentration of 0.8 mg/mL. Samples were made at 5 °C and a positive charge fraction of 0.6 and temperature was increased by 2 °C every 10 min to 35 °C. Data is plotted up to the transition to bulk phase separation. DLS data for bulk phase separation is not shown because DLS is unsuitable for characterizing bulk phase separation due to its dispersity, temporal instability, and inconsistent morphology.

S34. Figure S26. DLS as a function of temperature for ELP-PA C-term/ GFP(+36) at $f^+ = 0.6$

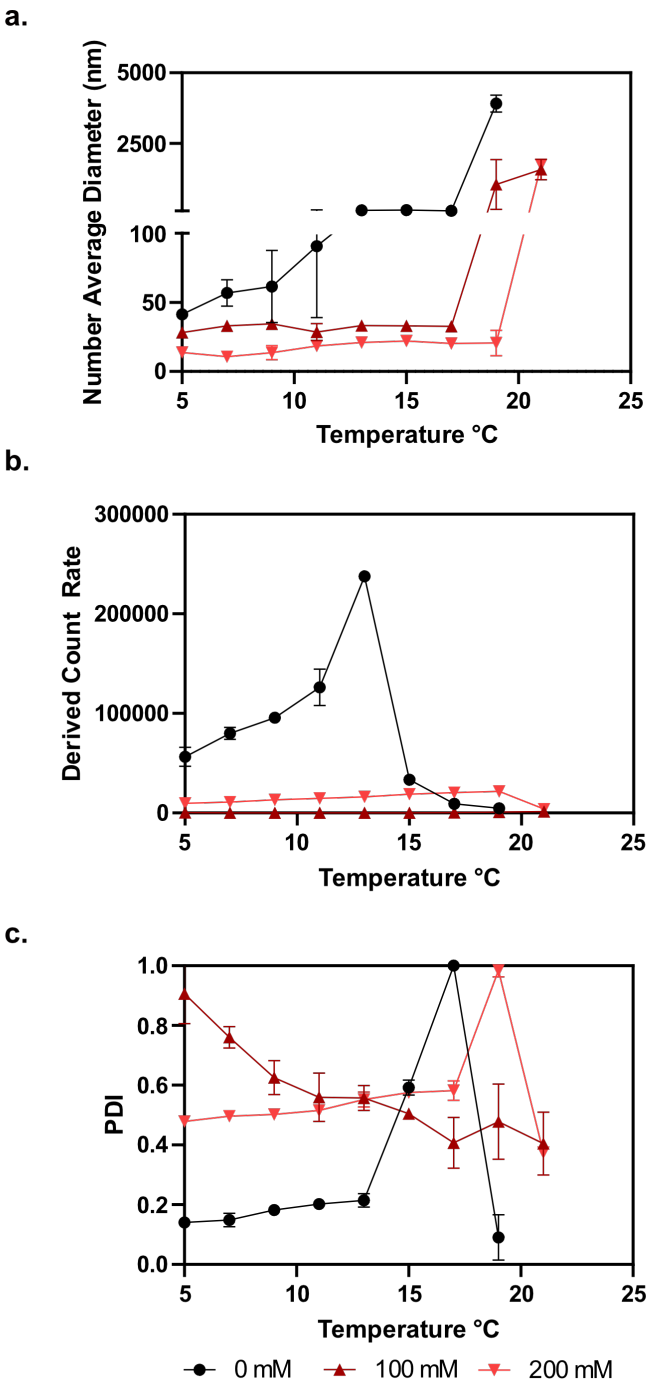

Figure S26. Number average diameter (a), derived count rate (b), and PDI (c) of ELP-PA C-term mixed with GFP(+36) at a total macromolecule concentration of 0.8 mg/mL. Samples were made at 5 °C and a positive charge fraction of 0.6 and temperature was increased by 2 °C every 10 min to 35 °C. Data is plotted up to the transition to bulk phase separation. DLS data for bulk phase separation is not shown because DLS is unsuitable for characterizing bulk phase separation due to its dispersity, temporal instability, and inconsistent morphology.

S35. References

1. Tang, N. C. & Chilkoti, A. Combinatorial codon scrambling enables scalable gene synthesis and amplification of repetitive proteins. *Nat. Mater.* **15**, 419–424 (2016).
2. Yeong, V., Werth, E. G., Brown, L. M. & Obermeyer, A. C. Formation of Biomolecular Condensates in Bacteria by Tuning Protein Electrostatics. *ACS Cent. Sci.* **6**, 2301–2310 (2020).
3. BARER, R. & JOSEPH, S. Refractometry of Living Cells : Part I. Basic Principles. *J. Cell Sci.* **s3-95**, 399–423 (1954).